TÉCNICO LISBOA

Estimation of Effective Diffusion Coefficients with Nernst-Planck equations in the Direct Borohydride-Peroxide Fuel Cell

Massimiliano Banini

Thesis to obtain the Master of Science Degree in

Energy Engineering and Management

Supervisors: Prof. Diogo Miguel Franco dos Santos

Prof. Vítor Manuel Geraldes Fernandes

Examination Committee

Chairperson: Prof. Luís Filipe Moreira Mendes

Supervisor: Prof. Diogo Miguel Franco dos Santos

Member of the Committee: Dr. Biljana Šljukić Paunković

December 2021

I declare that this document is an original work of my own authorship and that it fulfils all the requirements of the Code of Conduct and Good Practices of the *Universidade de Lisboa*.

Acknowledgements

Firstly, I have to sincerely acknowledge Dr. Diogo dos Santos for always being available for my questions and doubts, with patience and regularity, which helped me to deepen my knowledge about Direct Liquid Fuel Cells.

Secondly, I would like to thank Dr. Vitor Geraldes, which helped to develop the work with new insights that were not explored before.

I would like to mention also the help of Raisa Paes and Tiago Silva, which helped me to perform tests in the lab.

And last, but not least, I must thank my friends and university colleagues, that made my master experience unique and special.

Abstract

This work intends to develop a theoretical model for membranes for application in low-temperature liquid fuel cells, referring, particularly, to the direct borohydride-peroxide fuel cell (DBPFC), as a first step to create a numerical model. The DBPFC is based on the anodic oxidation of sodium borohydride ($NaBH_4$) in alkaline solution with the simultaneous cathodic reduction of hydrogen peroxide (H_2O_2) in acid media.

The model is mainly based on the Nernst-Planck equations, where all components of the system are considered to explain the passage of the ions through the membrane used. The latter is split into one section where there is a constant electric field due to the potential difference between the electrodes, and another section without it, but where there is a local difference of electric potential between the two sides of the membrane, i.e., the membrane potential.

The experiments performed allow investigating the mechanisms inside the membrane and finding the diffusivity of the components passing through it. A Python code was used to estimate “effective diffusion coefficients” of NaOH in Nafion N117, and obtaining a rough approximation of Na^+ to 9.82E-08 cm^2s^{-1}, and of OH^- to 1.04E-08 cm^2s^{-1}, at ambient temperature. The building of a more detailed diffusion function depending on temperature (for each ion involved) is the next step of the project purpose. This study aims to be a starting point to the creation of a numerical model where liquid solutions are involved, and thus suitable for modelling DBPFCs.

Keywords

liquid fuel cell, direct borohydride-peroxide fuel cell, diffusion coefficients, numerical model, Python

Resumo

Este trabalho pretende desenvolver um modelo teórico para membranas para aplicação em células de combustível líquidas de baixa temperatura, referindo-se, particularmente, à célula de combustível direta de borohidreto-peróxido (DBPFC), como um primeiro passo para a criação de um modelo numérico. A DBPFC é baseada na oxidação anódica do borohidreto de sódio ($NaBH_4$) em solução alcalina com a redução catódica simultânea do peróxido de hidrogénio (H_2O_2) em meio ácido.

Os ensaios são baseados principalmente nas equações de Nernst-Planck, onde todos os componentes do sistema são considerados para explicar a passagem dos iões através da membrana utilizada. Este último é dividido numa seção onde há um campo elétrico constante devido à diferença de potencial entre os elétrodos, e noutra seção sem ele, mas onde há uma diferença local de potencial elétrico entre os dois lados da membrana, ou seja, o potencial de membrana.

Os ensaios realizados permitem elucidar os mecanismos de transporte no interior da membrana e encontrar a difusividade dos componentes que a atravessam. Um código Python foi usado para fazer uma estimativa dos chamados “coeficientes de difusão efetivos” do NaOH em Nafion N117, e obter uma aproximação para o Na^+ (9,82E-08 cm^2s^{-1}), e para o OH^- (1,04E-08 cm^2s^{-1}), à temperatura ambiente. Este estudo pretende ser um ponto de partida para a criação de um modelo numérico onde estão envolvidas soluções líquidas e, portanto, adequado para a modelação de DBPFCs.

Palavras-chave

pilha de combustível líquido, pilha de combustível de borohidreto-peróxido, coeficientes de difusão, modelo numérico, Python

Table of Contents

List of Figures

List of Tables

List of Abbreviations

AEMs	anion-exchange membranes
CEMs	cation-exchange membranes
DBPFC	direct borohydride-peroxide fuel cell
HCl	hydrochloric acid
H_2O	water
H_2O_2	hydrogen peroxide
$NaBH_4$	sodium borohydride
$NaBO_2$	sodium metaborate
NaOH	sodium hydroxide
OCV	open-circuit voltage
PEMFC	proton-exchange membrane fuel cell
PMBI	pH-gradient-enabled microscale bipolar interface
SOFC	solid oxide fuel cell

List of Symbols

δ	membrane thickness [cm]
Ψ	membrane potential [V]
β	parameter used in Eq. 17 [V*mol/m^4]

List of Software

Ansys Fluent	Ansys Fluent is the industry-leading fluid simulation software known for its advanced physics modelling capabilities and industry leading accuracy.
Anaconda Navigator	Anaconda Navigator is a desktop graphical user interface (GUI) included in Anaconda® distribution that allows you to launch applications and easily manage conda packages, environments, and channels without using command-line commands. Navigator can search for packages on Anaconda.org or in a local Anaconda Repository. It allows to run the Spyder environment, where the Python (version 4.0.1) code is run.

Chapter 1

Introduction

1.1 Overview

This work intends to develop a numerical model for application in low-temperature liquid fuel cells, namely in the direct borohydride-peroxide fuel cell (DBPFC). This device uses fuel and oxidant that are liquid at room temperature, making it ideal for power generation in space and underwater applications, where O_2 gas is not easily available.

Besides the electrodes, the membrane separator is the main component to focus on the DBPFC, as it inhibits shorting between anode and cathode and the mixing of fuel and oxidant solutions. The promising high performance of DBPFCs is being hindered by the disparate pH requirements for the fuel oxidation (highly alkaline) and the oxidant reduction (highly acidic). Presently, cation-exchange membranes (CEMs) and anion-exchange membranes (AEMs) are used, but understanding the mechanism behind their behavior will also lead to an improvement of the recently proposed pH-gradient-enabled microscale bipolar interface (PMBI).

1.2 Motivation and Contents

In the laboratory development of direct borohydride-peroxide fuel cells (DBPFC), the membrane has been used until now as a black box, where the initially selected inputs lead to obtaining the fuel cell polarization and power density curves as outputs. So far, numerical models (and Computational Fluid Dynamic (CFD) models) for fuel cells have been mainly used for gaseous flows involved, as in the well-studied proton-exchange membrane fuel cell (PEMFC), but a working numerical model for liquid fuel cells is not available in the literature. This study aims to be a starting point to the creation of a corresponding model where liquid solutions are involved, and thus suitable for modelling DBPFCs.

A numerical model could give us some solutions/indications of the process occurring in the membrane, to better explain the passage of the ions through the membrane and to study some effects related to the crossover (for example, the crossover of borohydride from one compartment to the other decreases the efficiency of the system).

This thesis could give that input to further enhance the performance of the membrane, also for what will be studied in the near future, which is the development of pH-gradient-enabled microscale bipolar interface (PMBI).

Ion-selective membranes used for fuel cells can be:

- Cation Exchange Membrane (CEM)
- Anion Exchange Membrane (AEM)
- pH-gradient-enabled microscale bipolar interface (PMBI).

The latter is more specific because PMBI is supposed to be able to sustain the high pH difference on each side of the membrane. The reason is that the borohydride side works in alkaline media, and the hydrogen peroxide side works in acid media.

A numerical model could be very useful to do the analysis: it allows us to make a direct comparison between the different types of membranes, see which one seems more suitable, and what will be the advantages. The numerical model is enriched with the data obtained from the lab experiments, which allowed us to work with real data.

The numerical model for liquid fuel cells is the novelty of the present work. It will be a starting point to create an even more complex system taking care of all the variables involved, and it could lead in the future to the construction of a CFD model and an even optimized new 3D-printed direct borohydride fuel cell.

This thesis is composed of 4 chapters and 2 Annexes.

- Chapter 1 – Introduction
    - 1.1 – Overview
    - 1.2 – Motivations and Contents
    - 1.3 – State-of-the-Art
    - 1.4 – Preliminary study
        - 1.4.1 – Ansys Fluent modelling
- Chapter 2 –Materials and Methods
    - 2.1 – Lab equipment and test technique
    - 2.2 – Regression from the results
    - 2.3 – Theoretical model
        - 2.3.1 – Model creation
        - 2.3.2 – Forecast flux with constant initial concentration
        - 2.3.3 – Concentration profile and membrane potential profile inside the membrane
- Chapter 3 – Results and Discussion
    - 3.1 – NaOH-Nafion experiment
    - 3.2 – NaOH-Nafion data analysis
    - 3.3 – Diffusivities finder – Python code
- Chapter 4 – Conclusions and future work
- Annex A
    - A.1.1 – Concentration profile inside the membrane
    - A.1.2 – Membrane potential profile inside the membrane
    - A.1.3 – Alternative Membrane potential profile inside the membrane
- Annex B
    - B.2.1 – Python Code
    - B.2.2 – Python Code Explanation

1.3 State-of-the-Art

The State-of-the-Art of membranes in direct borohydride fuel cells is well organized in the book *Direct Liquid Fuel Cells: Fundamentals, Advances and Future* [1], thanks to the study and research of B. Šljukić and D.M.F. Santos.

Figure 1 shows a schematic drawing of a DBPFC, where there are two compartments divided by a membrane. On the left there is the anode side, in a highly alkaline environment, where the fuel oxidation (of the sodium borohydride) happens. On the right there is the cathode side, in a highly acidic environment, where the oxidant reduction happens. An external circuit allow the passage of electrons from the anode to the cathode side.

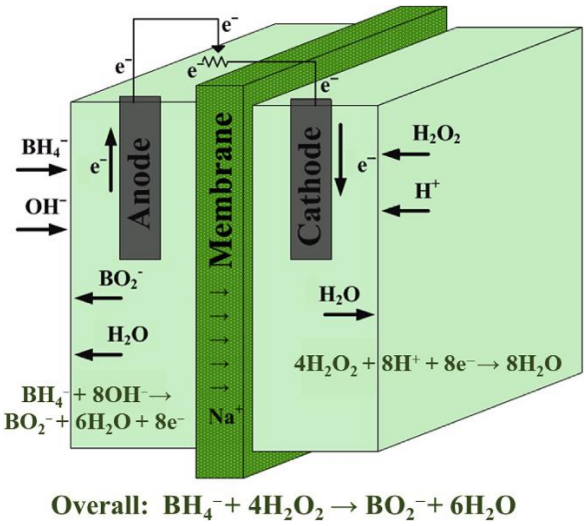

Figure 1 - Schematic illustration of a direct borohydride peroxide fuel cell (DBPFC) [2].

The membranes can be classified into 3 different types:

- Cation Exchange Membrane (CEM)
- Anion Exchange Membrane (AEM)
- pH-gradient-enabled microscale bipolar interface (PMBI).

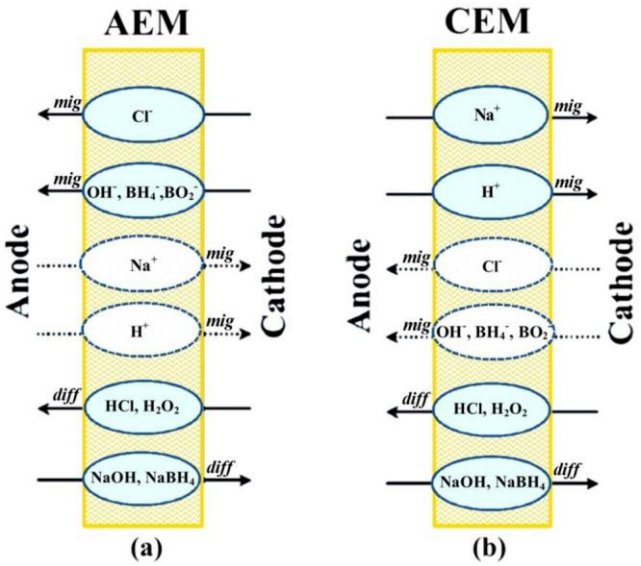

Figure 2 - Schematic illustration of the major migrative and diffusive fluxes across (a) anion and (b) cation exchange membranes used in direct borohydride/peroxide fuel cells (DBPFCs). Dotted lines show the type of ions that are blocked/hindered by the specific membrane. [3].

In Figure 2, the differences between AEM and CEM are shown, with the interaction of the membrane with positive ions, negative ions and neutral species.

Wang et al. recently described efficient pH-gradient-enabled microscale bipolar interfaces in direct borohydride fuel cells [4], including a microscale visualization of these new PMBI (see Figure 3).

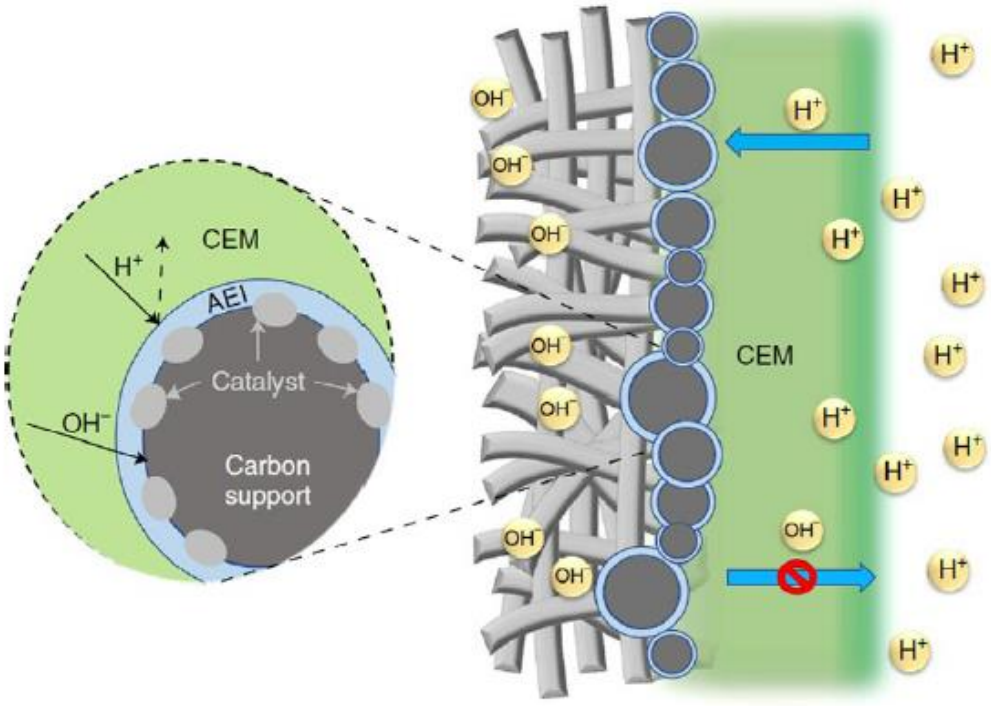

Figure 3 - General scheme of the processes occurring at the pH-gradient-enabled microscale bipolar interface. [4].

The generally accepted approach states that specific kinds of ions are blocked/hindered by the ion-selective membrane: so, for example in Nafion (CEM) the positive ions can pass easily through the membrane, while the negative ions cannot. In AEM, the mechanism is the opposite: negative ions can easily pass, while positive ions cannot.

Currently, in lab experiments, the membrane is considered as a black box, where only the input characteristics of the membrane are measured, and then the measured outputs are obtained for the fuel cell (Table 1).

Table 1 - Membrane inputs and outputs

Membrane inputs:	Membrane outputs:
• Molecular weight • Degree of hydrolysis • Thickness • Water uptake • Swelling ratio • Contact angle • Tensile strength • Oxidative stability • Ion exchange capacity • Ionic conductivity • Selectivity	• Polarization curve • Power density curve

The experiments are aimed to compare how a change in the membrane will affect the efficiency of the fuel cell, how will be the flow of ions through the membrane, etc.

The idea is to make a comparison between the different types of membranes and keep all the other components exactly the same. By that, direct information can be discovered on the effect of the membrane on fuel cell performance.

From lab tests on solutions and electrodes [5,6] the suggested optimized solutions for DBPFC are proposed: the anolyte solution has 1 M $NaBH_4$ + 4 M NaOH and the catholyte has 3 M H_2O_2 + 1 M HCl.

The pre-activation of the Nafion membrane is done in a NaOH solution, where H^+ ions inside the membrane are replaced with Na^+ ions.

At this point, the dissociation of NaOH in solution is highlighted in Eq. 1:

$$NaOH \leftrightarrows Na^+ + OH^- \quad (1)$$

(where the equilibrium is shifted to Na^+)

Then a solution of 1M $NaBH_4$ inside 4 M NaOH is created, where the $NaBH_4$ in solution is split into ions (Eq. 2):

$$NaBH_4 \leftrightarrows Na^+ + BH_4^- \quad (2)$$

(where the equilibrium is shifted to Na^+)

This solution is used as fuel in the anodic compartment. The fuel solution should be prepared before the

experiments, not too much in advance, to avoid the borohydride chemical hydrolysis.

So, the $NaBH_4$ overall complete oxidation is shown in Eq. 3:

$$Na^+ + BH_4^- + 8Na^+ + 8OH^- \rightarrow B(OH)_4^- + 4H_2O + 9\ Na^+ + 8e^- \quad (3)$$

8 Na^+ pass through the membrane, because $8e^-$ flow through the external circuit.

But there is the production of hydrogen gas inside, because of the partial hydrolysis of borohydride (Eq. 4):

$$BH_4^- + H_2O \rightarrow H_2 + BH_3OH^- \quad (4)$$

(and if H^+ pass from cathode to anode, more Na^+ has to pass for equilibrium)

So, the main reaction (considering that Na^+ does not react) is shown in Eq. 5:

$$BH_4^- + 8OH^- \rightarrow B(OH)_4^- + 4H_2O + 8e^- \quad (5)$$

While the unwanted side reaction is shown in Eq. 4.

So, the overall borohydride oxidation is written in Eq. 6:

$$BH_4^- + xH_2O \rightarrow B(OH)_4^- + (x\text{-}4)\ H_2O + (4 - \tfrac{x}{2})\ H_2 + xe^- \quad (6)$$

where "x" is the coulombic number. $1<x<8$, and using platinum electrodes corresponds to $x=4$.

These values of x can be obtained experimentally using typical electrochemical methods, like cyclic voltammetry, rotating disc electrode (RDE) or rotating ring-disk electrode (RRDE) measurements, and also by measuring the volume of hydrogen gas produced.

One of the current main problems for DBPFC is related to the species crossover, from one solution to the other: they decrease the efficiency of the whole cell, so minimizing them is necessary.

Three mass-transfer processes are occurring inside the electrolyte of a DBPFC: (electro-)migration, convection and diffusion.

- <u>(Electro-)Migration.</u> The voltage driving form is mostly caused by the voltage variation in the electrodes. By migration, cations go to the cathode and anions go to the anode. Until now electro-migration has been considered irrelevant compared with diffusion, for the low voltage process (maximum 2 volts). Normally, for a system where there is a very high ionic conductivity of the solutions (with a high electrolyte concentration) the effect of migration can be considered insignificant compared to the effect of diffusion, which is the most relevant process.
- <u>Convection</u>. It can be natural or forced convection. In case of forced convection, we have the input flow and the output flow. It could be referred to the situations where a recirculation (or a make-up flow) is present, to maintain stable the concentration in one solution (an example could be what happen inside PEMFC, but with a gaseous flow). Another example of forced convection could be when the flow is pushed against the membrane, for example when a filtration of a mixture must be obtained (for example to filter a gas like methane). So, in a forced convection, the velocity of the flow become a variable to consider in the mass transfer process. Instead, in the thesis experiments, only a natural convection is present. Here the convection is based on a

difference of density or temperature. The commonly used time is so low that it does not change the bulk concentrations, because a high volume of electrolyte solution on each side is considered. So, at the end of the experiment, the concentrations are the same. The concentrations are assumed to do not change. Due to this, convection has been considered irrelevant in comparison with the much higher weight in the process of diffusion. (The concentrations will not significantly change, so there will be no movement in the solutions due to the difference of density that will lead to natural convection inside the solutions).

- Diffusion. It is based on the concentration gradient in solution: in DBPFC, only cations can easily diffuse through the membrane if there is a cation exchange membrane (CEM).

Considering a proton exchange membrane (or cation exchange membrane) and consuming OH^- in the borohydride oxidation reaction (so the number of anions is decreasing on the anode side), to compensate for that, cations must be sent away (and the sodium cations go through the membrane from the anode side to the cathode side). So, this is the considered process, based on diffusion. Also, a concentration gradient of other species is present (like borohydride, for example, and by diffusion borohydride would tend to go to the other side, but a cation exchange membrane is present, so the membrane should not allow the passage of anions, only cations). Usually, for Nafion the typical borohydride permeability is known, which leads to the amount of borohydride crossover to the other side.

The membrane should not allow passing, but there is always some crossover of species with opposite charge (that should not pass a cation exchange membrane, but in fact, they pass because of the concentration gradient).

Na^+ is considered as the main species passing considering a Nafion membrane (or cations exchange membrane) and due to the diffusion effect (the concentration gradient) Na^+ will pass through the membrane and that will depend on the sodium diffusion coefficient in solution, and it will depend also on the diffusion coefficient inside the membrane (this information is sometimes given by the manufacturers).

For anion exchange membrane it will be different: Na^+ should not passage through the membrane. So, hydroxide ions (OH^-) can be considered, and it will tend to go to the other side much more (as well as borohydride), but from the cathode side there will probably be also some passage by diffusion of chloride ions (Cl^-, because there is hydrogen chloride on the cathode side, so Cl^- would probably pass to the anode side). The passage of Cl^- could be considered, because on the anode side borohydride and hydroxide are being consumed, so there is a decrease in their concentration with time, so there is so much quantity to go to the other side.

In CEM and AEM there is also a crossover of neutral species (water and H_2O_2), and they are also unwanted.

If water passing is not be so important, the passage of H_2O_2 is a problem, because it is a strong oxidant (water is in large percentage in both solutions, but peroxide is only in acid solution, so it tends to pass

through the membrane to go to the other side)

Two effects are the consequences of this H_2O_2 passage:

1) loss of reactants
2) BH_4^- reacts suddenly, disappearing, because it reacts with H^+ (that is created from the H_2O_2 passed, which dissociates: $H_2O_2 \leftrightarrows HO_2^- + H^+$). H_2O_2 is a very strong oxidant: it gives oxygen very easily, this would quickly oxidize borohydride.

For diffusion, water does not pass (concentration of water is almost the same in both solutions) but H_2O_2 crossover is difficult to stop.

A loss of H_2O_2 in the acid solution leads to a loss of BH_4- in the alkaline solutions: there is an oxidation of BH_4- in the alkaline solution.

A high potential difference between the two electrodes in the fuel cell is desirable, to have a higher cell voltage, but this passage of H_2O_2 to the alkaline solution will tend to have a faster balance in the pH of the solutions, so the cell voltage will be lower. This happens because of the dissociation (in Eq. 7):

$$H_2O_2 \leftrightarrows HO_2^- + H^+ \quad (7)$$

will also bring H^+ passing through the membrane (from acid solution to alkaline solution. It will pass like Na^+, but in the opposite direction), and this H^+ will lead to a consumption of $BH4^-$, and a decrease of the pH of the anode (alkaline solution).H_2O_2 reacts directly with BH_4- and both are consumed in this chemical process: no electricity is generated.

In a different situation, two alkaline solutions can be used on the two sides of the membranes (so no acid solution is involved). But this leads to a new problem: if both solutions are alkaline, there will be too much production of O_2 (that can be seen as the formation of gas in the volumes), because H_2O_2 stability in alkaline media is much lower (Eq. 8):

$$H_2O_2 \rightarrow H_2O + ½\ O_2 \quad (8)$$

Reducing this O_2 (and not H_2O_2) losing the potential of the electrodes is reduced, i.e., the cathode potential will be lower. So, different species and different solutions, have pros and cons in each membrane.

Plotting the current density over time (Figure 4), there is the first steep part of the curve (at high voltage, near the OCV, around 2 V) where there is a pure charge control.

Species next to the electrode are suddenly consumed when the system “leaves” the OCV. Once the resistance is no longer infinite, the species start to be consumed near the electrode. So, it is only infinite at open-circuit conditions.

At low voltage (high current density) there is a pure mass transfer control (also called diffusion control).

In the middle of the curve, there is a mixed control between the two regimes.

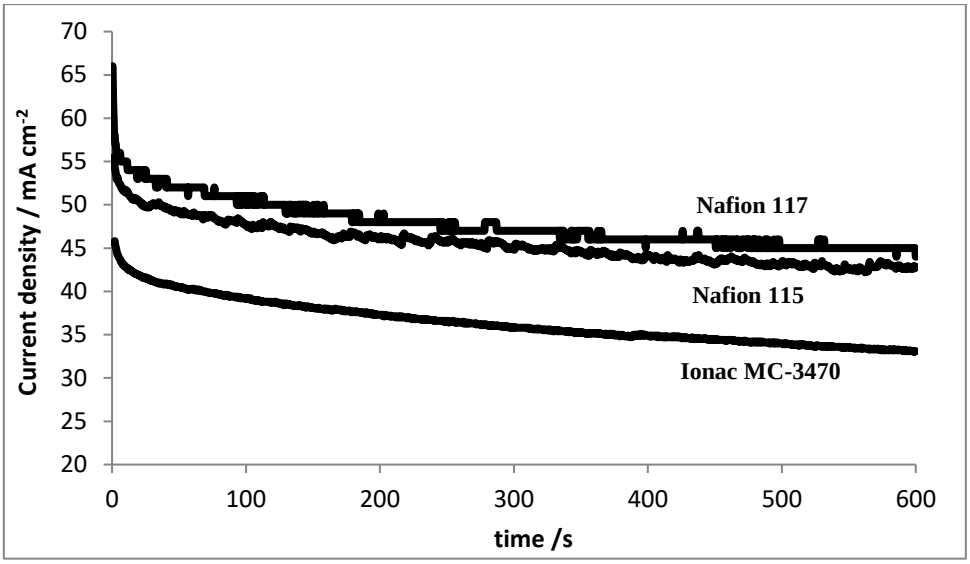

Figure 4 - Example of current density decay over time for 3 different CEMs [5].

With no pressure change, no different temperature, no concentration change (due to movement created from different densities), convection inside the membrane will not occur. Only considering the flow, the convection can be considered. Only after the first part, the diffusion will start to work.

The curve decreases with time because there is no feeding. Otherwise, with a make-up flow (or a recirculation) after the first part the curve would remain constant. Catalyst deactivation or membrane failure can also lead to that.

From Figure 4, it can be seen that if Nafion117 reaches current densities of 50 $mAcm^{-2}$, with a bipolar membrane it could be expected the DBPFC to reach about 250 $mAcm^{-2}$. Other research centers have the same expectation, but are performing experiments with recirculation/make-up flow, to get a stable curve after the first seconds.

The lab tests are performed with power less than the peak power (so in the left part of the polarization curve), otherwise the fuel cell would be quickly discharged. So, for example, instead of working with 0.8 V (corresponding to the potential at peak power), 1 V is used. And this is only a single cell test, but usually fuel cells stacks are used. So, if 12 V are needed in the fuel cell, 12 fuel cells (working at 1 V each) will have the total voltage needed.

Some “homemade” membranes (PVA/PEO/PVP, PVA/PEO/PVP-SGO-1, PVA/PEO/PVP-SGO-3) have been already tested as an alternative to expensive Nafion [7]. Similar tests are performed also in this article [2]

Other commercial membranes (CMI-7000S and AMI-7001S) were tested [3], so all the membranes

tested can be resumed in the following list:

1) Commercial Nafion©
2) poly (vinyl alcohol) (PVA) (doped with sulfonated graphene oxide (SGO))
3) poly (ethylene oxide) (PEO)
4) poly (vinyl pyrrolidone) (PVP)
5) PVA/PEO/PVP-SGO-1 (1 wt%)
6) PVA/PEO/PVP-SGO-3 (3 wt%)
7) PVA/PEO/PVP

Non-perfluorinated based polymers, like poly (benzimidazole) (PBI), poly (ether ether-ketone) (PEEK), poly (styrene) (PS) and poly (arylene ether sulfone) (PSU), are the polymers most studied, utilized to make new alternative membranes: from the technological and commercial point of view, it is more desirable to use simpler and cheaper polymers, such as poly (vinyl alcohol) (PVA), to make polymer blends than developing new complex polymers or modifying commercial membranes. [7]

1.4 Preliminary study

An initial path to building a CFD model has been studied: the idea was to start to adapt a working code for solid oxide fuel cell (SOFC) available online.

Different publications regarding the SOFC numerical model are available in the literature [8-20] and a free code is available online [21,22].

In the most complete document (written in 2016) [20], the open-source model for SOFC started to be created, but during the last 5 years, no updates have been given. The idea was to make it flexible to all fuel cell types, but of course, it depends on the people working on it and if they want to publish their modification for the code for free.

SOFC is not so similar to DBPFC. Instead, PEMFC could be used to have a better starting point: PEMFC would be closer to DBPFC because the membrane is similar, whereas in SOFC it is a ceramic (solid oxide). In a PEMFC, a PEM (polymer electrolyte membrane) is used to separate each compartment, like in the DBPFC.

Different studies on PEMFC numerical models are available online [23-28], so it could have been easier starting to work with some working code to adapt to DBPFC, but collaboration with Jean-Paul Kone referring to his article [26] and his code was not possible.

A resume of different paths to create a model is analyzed in Table 2:

Table 2 - Resume of different paths to create a model

1) Language: C++. Software: OpenFOAM
It is possible to adapt the softFOAM.c code available online (made for SOFC) also for the DBPFC, but many forks and variants of the software have been present in the last years (above all the different business approaches of OpenFOAM.com and OpenFOAM.org), and the last contribution to the code is dated in 2016. Many open-source codes suffer from a lack of documentation and support: having more than 10 different variants (probably more) of the same code, will create a lot of instability and adaptability issues.
2) Language: Python It is possible to develop a model on Python, adapting the code of PEMFC [29]
3) Software: Comsol® The commercial software Comsol® has a specific module for “fuel cell and electrolyzer” [30]. Only a free version of 15 days is available, otherwise the software could be bought with an expensive annual subscription (998 euro for the basic software + 498 euro for the specific module) or with a perpetual license (1995 euro for the basic software + 995 euro for the specific module).

4) Software: Ansys Fluent®

Ansys is a commercial software, with a free version for Academic Purposes (with limitations on nodes and operations), and it has an Advanced Add-On for PEMFC. Tutorial and working 3D model [31] are available online, to adapt to DBPFC.

5) Software: Matlab®

The commercial software Matlab® has a "Fuel Cell Stack Module" for generic Fuel Cell [32], that could be adapted for DBPFC.

1.4.1 Ansys Fluent modelling

After the initial research, the possibility to develop a model with Ansys Fluent was investigated.

The Ansys Student license has only these problem size limits [33]:

- Structural Physics: 128K nodes/elements
- Fluid physics: 512K cells/nodes

The difficulties encountered with the development of this model were:

- The simulation of new materials (like $NaBH_4$), not present in Ansys material database library, to put in the new mixture/solutions of the Fuel Cell
- The missing parameters from lab experiments that the software requires to run (only a few of all the characteristics of the material/solutions inside the DBPFC are known, and having them as much close as possible to have realistic results from the software forecasting)
- The missing data about the membranes to simulate (a complete knowledge of the correlations of the membrane properties with the mechanism occurring inside is missing)
- PEMFC module works mainly on gases, using only liquids affects the UDS (user-defined scalar, a function that can calculate advection and diffusion of a defined scalar): the properties of the fuel cell mixture follow the laws of gases and other user-defined functions, so the module could not be feasible for liquid fuel cell
- The GDL (Gas Diffusion Layer) is mandatory for PEMFC because it plays a vital role in its operations, and it is not possible to delete or neglect it unless creating a completely different module

But, above all, the most critical parameter for the simulation is the diffusivity inside the membrane: in the literature there are very few references for Nafion® membranes [33, 34], and no references for the home-made membranes. Without knowing the diffusivities inside the membranes, a numerical model cannot be run properly.

Chapter 2

Materials and Methods

2.1 Lab equipment and test technique

The lab has single direct borohydride fuel cells, where a membrane is separating the two compartments. On one side there is the borohydride solution (where the borohydride is oxidized in the anode), and on the other side there is a hydrogen-peroxide solution (where H_2O_2 is reduced). This work will consider a model electrode (like platinum) for both reactions, and it will focus on the membrane.

The present work does not involve the deposition of any layer of catalyst on the surface of the membranes: this is the procedure to prepare a complete system, but the focus of this dissertation is on the fundamental studies. The electrodes are simply placed close to the membrane (without depositing anything). Electrodes may be in direct contact, but they are usually almost touching. Deposition of layers on the membrane will make the latter unusable for further studies: instead, the focus is only on making a direct comparison between different materials, and being able to reuse them for various tests.

In a real membrane-electrode-assembly, the catalytic ink is painted or sprayed on each side of the fragile membrane, and then the fuel cell is used like that. But this is against our goal, where only a limited number of membranes are available (due to their cost). Moreover, for fundamental research, the same membrane is re-used for different studies. After usage, the membrane gets washed properly, stored, and then it can be used again to test different materials. This is possible only because the materials tested are very close to the membrane, but not painted on it: that is why it is possible to take the electrode out, store the membrane and use it again. Painting it on the catalyst will block the recycling/reuse of the membrane.

The membrane is as important as the concentrations in the two compartments. In solution there is only ionic conduction, and the electrical contacts are only between the electrodes and the potentiostat. The ionic diffusion depends on both concentration difference (between compartments) and electro-migration, due to the membrane potential created and the constant electric field in the vicinity of the electrodes.

In the electrodes, there should not be a release of gases, but in practice, there is always some decomposition of BH_4- and H_2O_2, forming H_2 and O_2, respectively.

In a DBPFC, H_2O_2 is used as liquid oxidant instead of the typical oxygen used in most fuel cells (Eq. 9), like the PEMFC. In this case, there is the direct reduction of the H_2O_2 (Eq. 10).

$$O_2 + 4H^+ + 4e^- \rightarrow 2H_2O \qquad E^0=1.23V \text{ vs. SHE} \tag{9}$$

$$H_2O_2 + 2H^+ + 2e^- \rightarrow 2H_2O \qquad E^0=1.77V \text{ vs. SHE} \tag{10}$$

H_2O_2 reduction occurs at more positive potentials, allowing higher cell voltages, and consequently higher power than with only O_2.

The theoretical energy density of this system is 1 $kWhkg^{-1}$: the problem is normally related to the high pH difference, which is why proper membranes are needed.

An aqueous alkaline solution of borohydride and an aqueous acid solution of H_2O_2 are used; that allows the use of this fuel cell in places where O_2 is not available, like in space or underwater

The DBPFC is formed by two compartments when around 100 mL of solution each can be poured (leaving some space on the top just in case some gases are formed, so they will be filled up only with 75 mL each). There are these metallic electrodes inside the two solutions: the two compartments are closed together (with the membrane and some rubber sealings in the middle, to avoid liquid leakage outside), and the fuel cell is ready.

Figures [5-11] show the main dimensions and the materials of the complete fuel cell.

Figure 5 - Solutions compartment, with rubber sealing to avoid liquid leakage. The chosen membrane will be put in the middle. Electrodes are visible inside the compartments.

Figure 6 – Average distance between electrodes: 3 cm. Minimum distance 2.5 cm, maximum distance 4.0 cm.

Figure 7 - Average distance between electrodes: 3 cm. Minimum distance 2.5 cm, maximum distance 4.0 cm.

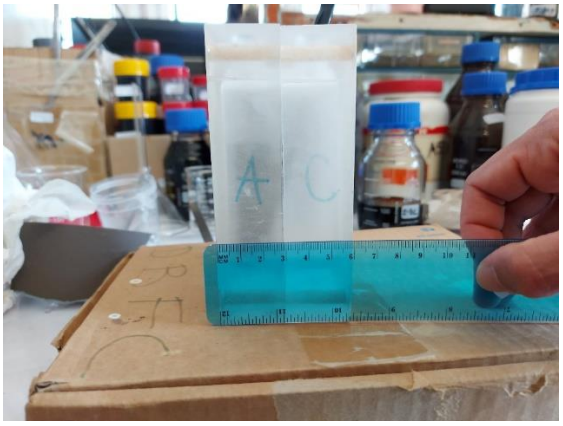

Figure 8 - 6.0 cm length (3.0 for each compartment).

Figure 9 - Width: 10,5 cm (for each compartment).

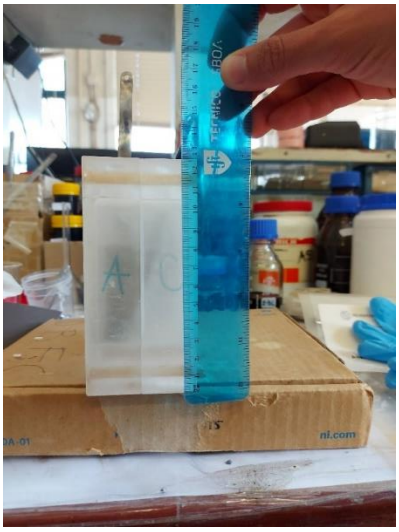

Figure 10 - Height: 12,5 cm each compartment.

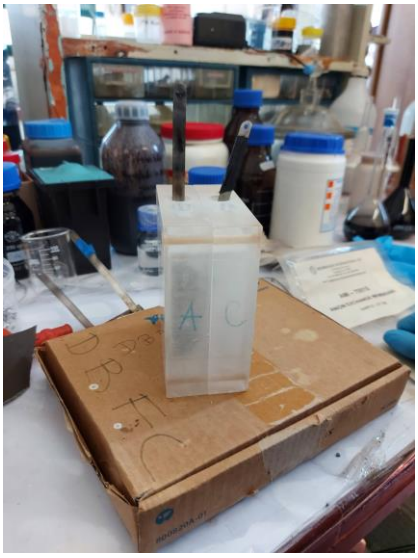

Figure 11 - Complete Fuel Cell set: from the Anode and the Cathode, they are the Electrodes to connect to the outside electrical system.

The idea is to change the type of membrane, so anion exchange membranes (AEM), cation-exchange membranes (CEM), and bi-polar membranes (BPM) can be compared with the same conditions.

Most research on borohydride fuel cells is normally focused on the materials that are being tested as anode or cathode for the fuel cell. Fundamental studies are made with those materials (like some basic electrochemistry studies to understand how they act as a catalyst either for the borohydride oxidation or for the hydrogen peroxide reduction, or for oxygen reduction also), and then tests are performed on that simple fuel cell.

In the case of Nafion membranes, a “pre-activation” before the test is needed: the H^+ of the commercial

membrane is replaced with Na^+, storing them in a NaCl solution.

What is the approach followed for the fuel cell testing? Different cell voltages are imposed, the currents (that are passing through the fuel cell) are measured, and by that a polarization curve and the power density curve are built. This allows a comparison of those with the data shown already in the literature.

On fuel cell testing, there is an initial potential difference between electrodes (the so-called open-circuit voltage) with an infinite resistance between them (so that no current is passing in the system). Starting decreasing the resistance between the electrodes, the electrons start to flow spontaneously.

Decreasing the resistance means decreasing the potential between them (moving closer to the electrodes). The only way to make the potential get closer is to pass electrons from one side to the other: that is how the potential between them decreases. If no resistance is put between the electrodes, their potential difference would decrease until being almost null. So, during the fuel cell test there is a spontaneous electrons flow.

For electrolyzers it is different: it is not a spontaneous process, and to generate an electron flow a higher potential is needed. The potentials on each electrode are put more apart and that will force electrons to go from the more positive side to the more negative side. It is a different process, but it is the same experimental approach: imposing cell voltages and then checking the currents generated from that.

The membranes can be chemically and mechanically fragile, so only certain currents are recorded, because after high currents they do not behave well. So, the polarization curve and the power density curves are just recorded until the peak power (avoiding higher currents).

Normally with Nafion© membranes (benchmark commercial membranes), it is possible to get almost the full power density curve (passing the peak, the curve decreases, without the need to reach the zero-power point). In the homemade membrane, only the peak is reached, because recording a complete curve could damage the membrane itself (due to the excessively high currents), making it unusable again.

A comparison of membranes using platinum electrodes (as a model electrode) is made, while in literature normally only Nafion membranes are used to compare the catalysts (the electrodes/electrocatalysts). In the lab the same Nafion membrane is used, comparing directly each different electro-catalyst and the different power density curves obtained in the fuel cell.

All the tests are performed with the same concentration. The first point is at no current passing in the cell, so the maximum cell voltage is called the open-circuit voltage (OCV), which is normally around 2 volts for this DBPFC. So, the start is with 2 V and 0 current.

The value of the resistance between the two electrodes is then decreased: it was an infinite resistance, and then it is a little bit lower. So, now the system is closed between the electrodes, and the connection has a high resistance. Closing the circuit, electrons start to flow spontaneously from the anode side to the cathode side: with this flow, the current starts increasing, and the cell voltage between them starts getting lower. So, they are becoming not so apart: one is losing charge, the other is receiving charge.

Usually, the test starts with a cell voltage of 2.0 V, and then it is decreased with every slide of 5 mV, till

0.5 V or 0.4 V, that is after the peak power density (normally the peak power occurs at 0.6-0.7 V). All of this is measured and controlled thanks to the usage of a potentiostat.

The initial high current stabilizes after the first seconds, so the current value is recorded after 30 seconds, and then the current point for 1.90 V is recorded. The same procedure is repeated for the following values, to create the polarization curve. After that, the power density curve can be found just by calculation (multiplying the current obtained at each applied cell voltage).

2.2 Regression from the results

Seeing the impossibilities to forecast new outputs without knowing the governing equations inside the membrane (and the relations between inputs and outputs), a regression from the results could bring new insights. Examples of polarization curves (Figure 12) and power density curves (Figure 13) are presented.

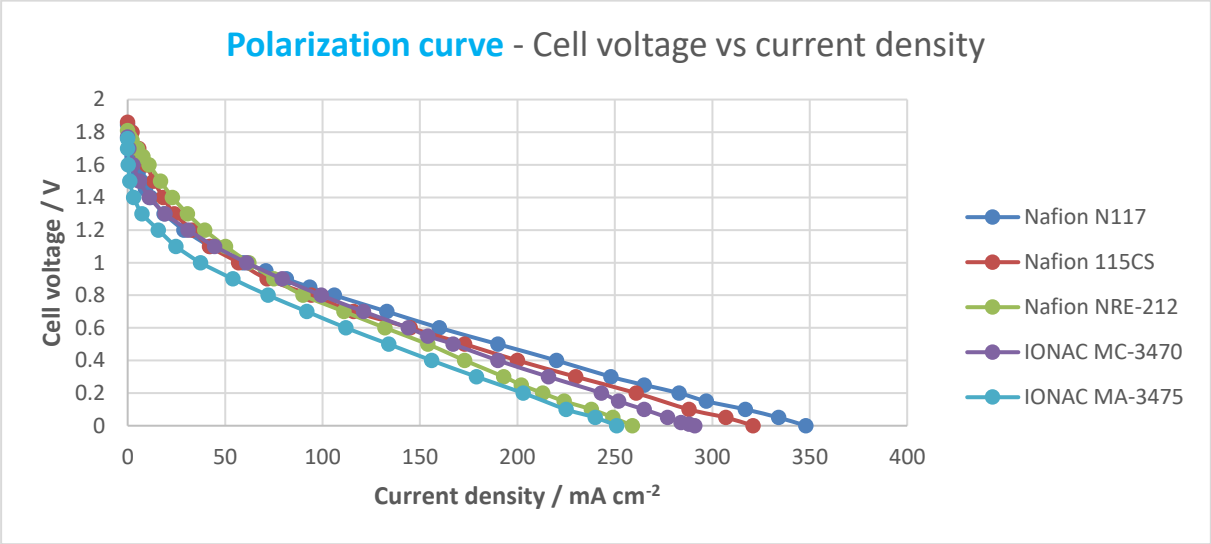

Figure 12 – Polarization curves recorded for DBPFCs using 5 different commercial cation-exchange membranes. Curves plotted with data taken from Santos and Sequeira [5].

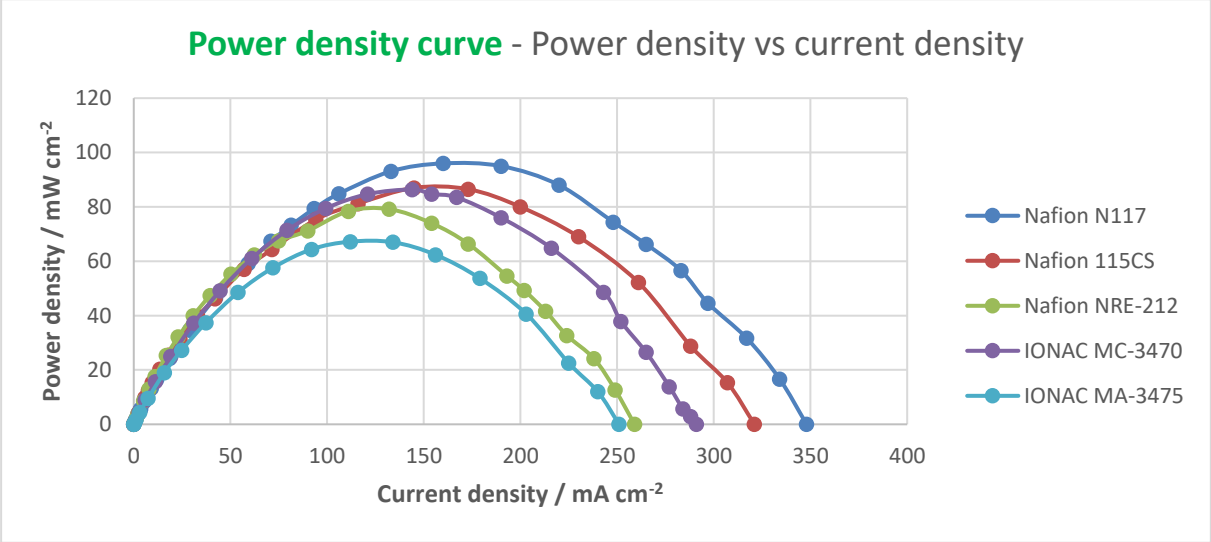

Figure 13 – Power density curves recorded for DBPFCs using 5 different commercial cation-exchange membranes. Curves plotted with data taken from Santos and Sequeira [5].

Seeing that the two main outputs (the polarization curve and the power density curve) are depending on the cell voltage, the objective function (that connects the cell voltage input with the outputs) can be extrapolated.

In this way, a system of equations for each membrane can be built (Table 3), to minimize the percentile

error and have a forecast of the results:

Table 3 - Equation's variables explanation.

$y= A*x^3 + B*x^2 + C*x + D$
y= current density [mA/cm^2]
x= cell voltage [V]
P= Power density [mW/cm^2]
P [mW/cm^2] = x [V] * y [mA/cm^2]

In Table 4-8 are shown the correlations found:

Table 4 - Regression for Nafion N117.

Voltage Range		Coefficients				Error
Min [V]	**Max [V]**	**A**	**B**	**C**	**D**	**Current Density Max ERROR [%]**
0.00	0.85	-43.211	119.17	-375.36	352.45	0.63%
0.85	1.10	869.18	-2351	1888	-346.71	0.81%
1.10	1.55	-92.749	504.74	-926.19	573.66	0.82%

Table 5 - Regression for Nafion 115CS.

Voltage Range		Coefficients				Error
Min [V]	**Max [V]**	**A**	**B**	**C**	**D**	**Current Density Max ERROR [%]**
0.00	0.60	-11.765	50.371	-320.56	321.78	0.77%
0.40	0.80	683.33	-1162.9	365.6	195.97	0.49%
0.50	0.90	8.3333	109.64	-419.83	354.7	1.21%
0.90	1.50	-30.556	222.98	-497.33	361.01	2.58%
1.50	1.80	38.333	-177.13	233.15	-67.047	1.48%

Table 6 - Regression for Nafion NRE-212.

Voltage Range		Coefficients				Error
Min [V]	Max [V]	A	B	C	D	Current Density Max ERROR [%]
0.00	0.80	-117.29	162.2	-270.8	262.27	0.86%
0.80	1.50	2.7778	60.833	-255.68	254.1	0.46%
1.30	1.65	-196.17	899.54	-1432.4	803.59	0.55%
1.60	1.75	0	19.375	-123.13	158.39	0.95%

Table 7 - Regression for IONAC MC-3470.

Voltage Range		Coefficients				Error
Min [V]	Max [V]	A	B	C	D	Current Density Max ERROR [%]
0.00	0.40	-321.06	156.38	-261.29	289.84	0.71%
0.40	1.20	60.66	-76.046	-203.38	279.73	0.62%
1.20	1.60	-150.83	775.79	-1349.9	794.38	0.46%

Table 8 - Regression for IONAC MA-3475.

Voltage Range		Coefficients				Error
Min [V]	Max [V]	A	B	C	D	Current Density Max ERROR [%]
0.00	0.40	-494.54	377.46	-318.7	254.59	0.50%
0.40	0.80	1E-10	42.857	-261.43	253.77	0.30%
0.50	0.90	3E-10	57.143	-280	259.66	0.37%
0.90	1.30	-283.33	1077.9	-1448	690.68	0.91%
1.30	1.70	-120	606	-1021.4	574.64	1.08%

All the R-squared values of the trend were near 1, and only third-order equations are used to avoid overfitting of the results (that could happen when using equations with a superior order).

The drawback of this method is that only the same results of the experiment done can be predicted (at T=25°C and $p=p_{atm}$=1atm), and new membranes cannot be predicted (without new lab tests).

Having instead much more data with different membranes and conditions, could help to enhance the possibilities of this method, which at one point could be also be upgraded with Machine Learning and Neural Networks. Realistically, thousands of different tests are not possible to be performed in a short time and without great expense.

2.3 Theoretical Model

2.3.1 Model creation

The model is mainly based on the Nernst-Planck equations (Eq. 11 and 12), where all components of the system are considered to explain the passage of the ions through the membrane used.

$$N^+ = -D^+ \frac{dC_S(x)}{dx} - C_S D^+ \frac{F}{R*T} \frac{d\Psi(x)}{dx} \quad (11)$$

$$N^- = -D^- \frac{dC_S(x)}{dx} + C_S D^- \frac{F}{R*T} \frac{d\Psi(x)}{dx} \quad (12)$$

With the salt concentration expressed in Eq. 13:

$$C_s = z^+ * C^+ = z^- * C^- \quad (13)$$

N^+ = flux of positive ions through the membrane [mol/(cm^{2}s)]

N^- = flux of negative ions through the membrane [mol/(cm^{2}s)]

D^+ = diffusivity of positive ions inside the membrane [cm^2/s]

D^- = diffusivity of negative ions inside the membrane [cm^2/s]

C_s = concentration of molecule inside the membrane [mol/cm^3]. It is a function of x.

C^+ = concentration of positive ions inside the membrane [mol/cm^3]

C^- = concentration of negative ions inside the membrane [mol/cm^3]

z^+ = valence of positive ions [-]

z^- = valence of negative ions [-]

x = x-axis position inside the membrane thickness [cm] → $0 \leq x \leq \delta$

δ = membrane thickness [cm]

F = 96485.3365 [C/mol] Faraday Constant

R = 8.31446261815324 [J/(mol*K)] Gas Constant

T = Temperature [K]

Ψ [V] = membrane potential. It is a function of x.

Only the diffusion (first term) and the electro-potential/migration (second term) of the equations are considered, and not the convection term: in the fuel cell there is neither recirculation nor convection inside.

To keep the electroneutrality of solutions (Donnan's equilibrium in Eq. 14), the flux of positive ions N^+ is equal to the flux of negative ions N^- (Eq. 15 and 16). So:

$$N^+ = N^- = N \quad (14)$$

$$N = -D^{+}\frac{dC_s(x)}{dx} - C_s D^{+}\frac{F}{R*T}\frac{d\Psi(x)}{dx} \quad (15)$$

$$N = -D^{-}\frac{dC_s(x)}{dx} + C_s D^{-}\frac{F}{R*T}\frac{d\Psi(x)}{dx} \quad (16)$$

A new parameter β is defined (Eq. 17):

$$\beta\left[\frac{V*mol}{cm^4}\right] = \frac{R\left[\frac{J}{mol*K}\right]*T[K]*N\left[\frac{mol}{cm^2*s}\right]}{2*F\left[\frac{C}{mol}\right]} * \left[\frac{D^{+}\left[\frac{cm^2}{s}\right]-D^{-}\left[\frac{cm^2}{s}\right]}{D^{+}\left[\frac{cm^2}{s}\right]*D^{-}\left[\frac{cm^2}{s}\right]}\right] \quad (17)$$

The boundary condition at the edges of the membrane are expressed in Eqs. 18-23:

$$C_s(0) = C_{s0} \quad (18)$$

$$C_s(\delta) = C_{s1} \quad (19)$$

$$\Delta C_s = C_{s1} - C_{s0} \quad (20)$$

$$\Psi(0) = \Psi_0 \quad (21)$$

$$\Psi(\delta) = \Psi_1 \quad (22)$$

$$\Delta\Psi = \Psi_1 - \Psi_0 \quad (23)$$

Resolving the differential equations, the equations of the membrane potential (Eq. 24) and the equations of the concentrations (Eq. 25), can be obtained:

$$\Psi(x) = \Psi_0 + \frac{\beta}{A} * \left[\ln\left(\frac{C_{s0}}{C_{s0} - A*x}\right)\right] \quad (24)$$

$$C_s(x) = C_{s0} - A * x \quad (25)$$

(The whole derivations are described in Annex A.1)

With the parameter *A* defined as Eq. 26:

$$A = \frac{N*(D^{-}+D^{+})}{2*D^{+}*D^{-}} \quad (26)$$

An additional linearization of the model (Eq. 27 and 28) can be proposed, considering directly the edges of the membrane with the boundary conditions:

$$\Delta\Psi = \frac{\beta}{A} * \left[\ln\left(\frac{C_{s0}}{C_{s0} - A*\delta}\right)\right] \quad (27)$$

$$\Delta C_s = C_{s0} - A * \delta \quad (28)$$

A linearization of the Nernst-Planck equations (Eq. 29 and 30) will be expressed as:

$$N = -D^{+}\frac{\Delta C_s}{\Delta x} - C_{s1} D^{+}\frac{F}{R*T}\frac{\Delta\Psi}{\Delta x} \quad (29)$$

$$N = -D^{-}\frac{\Delta C_s}{\Delta x} + C_{s1} D^{-}\frac{F}{R*T}\frac{\Delta\Psi}{\Delta x} \quad (30)$$

Three scenarios are possible:

- If $D^{+} = D^{-}$, there is no electrical potential gradient
- If $D^{+} > D^{-}$, the electrical potential will retard the cations and accelerate the anions

- If $D^+ < D^-$, the electrical potential will accelerate cations and retard the anions

The DBPFC system is split into one section where there is a constant electric field due to the potential difference between the electrodes (where the current is different from zero), and another section without it (where the current is equal to zero), but where there is a local difference of electric potential between the two sides of the membrane, i.e., the membrane potential (Figure 12). This effect is created by the different diffusivity of the ions inside the membrane. To keep the electroneutrality (Donnan's equilibrium in the solutions) in the fuel cell compartments, the system uses a mechanism where the faster ions are slowed down and the slower ions are accelerated, to allow both oppositely charged ions to pass.

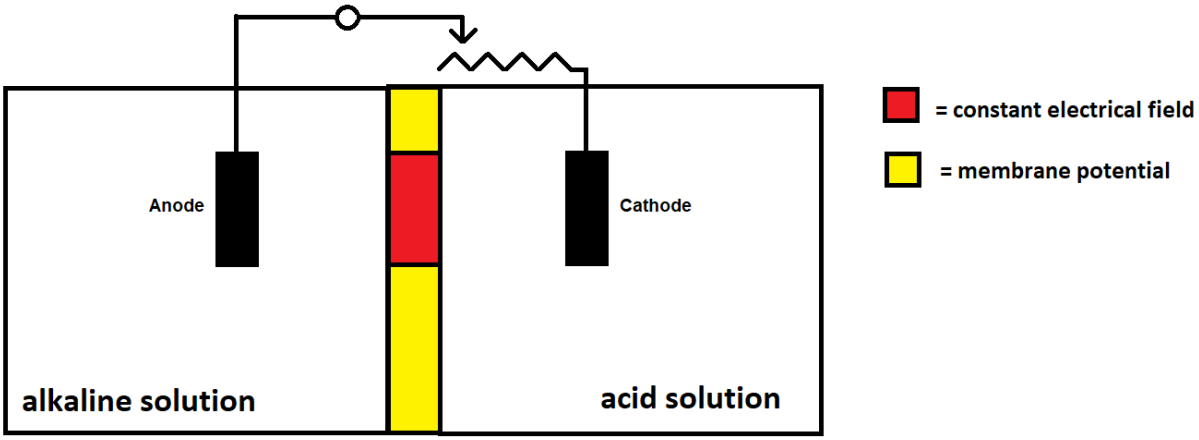

Figure 14 - Membrane sections: in the red sections (at the same level of the electrodes) we have a constant electrical field (current different from zero), while in the yellow part we have only the membrane potential (with current equal to zero).

The innovative part of the model is that the passage of the ions is considered individually for each species involved. Each sub-system is considered to work independently based on the different concentrations on each side of the membrane and the specific membrane potential created. The total membrane potential (of the whole DBPFC system) is, consequently, the overlayed effect of all sub-systems, according to the superposition principle. This model is an upgrade to the generally accepted approach where specific kinds of ions are blocked/hindered by the ion-selective membrane [2].

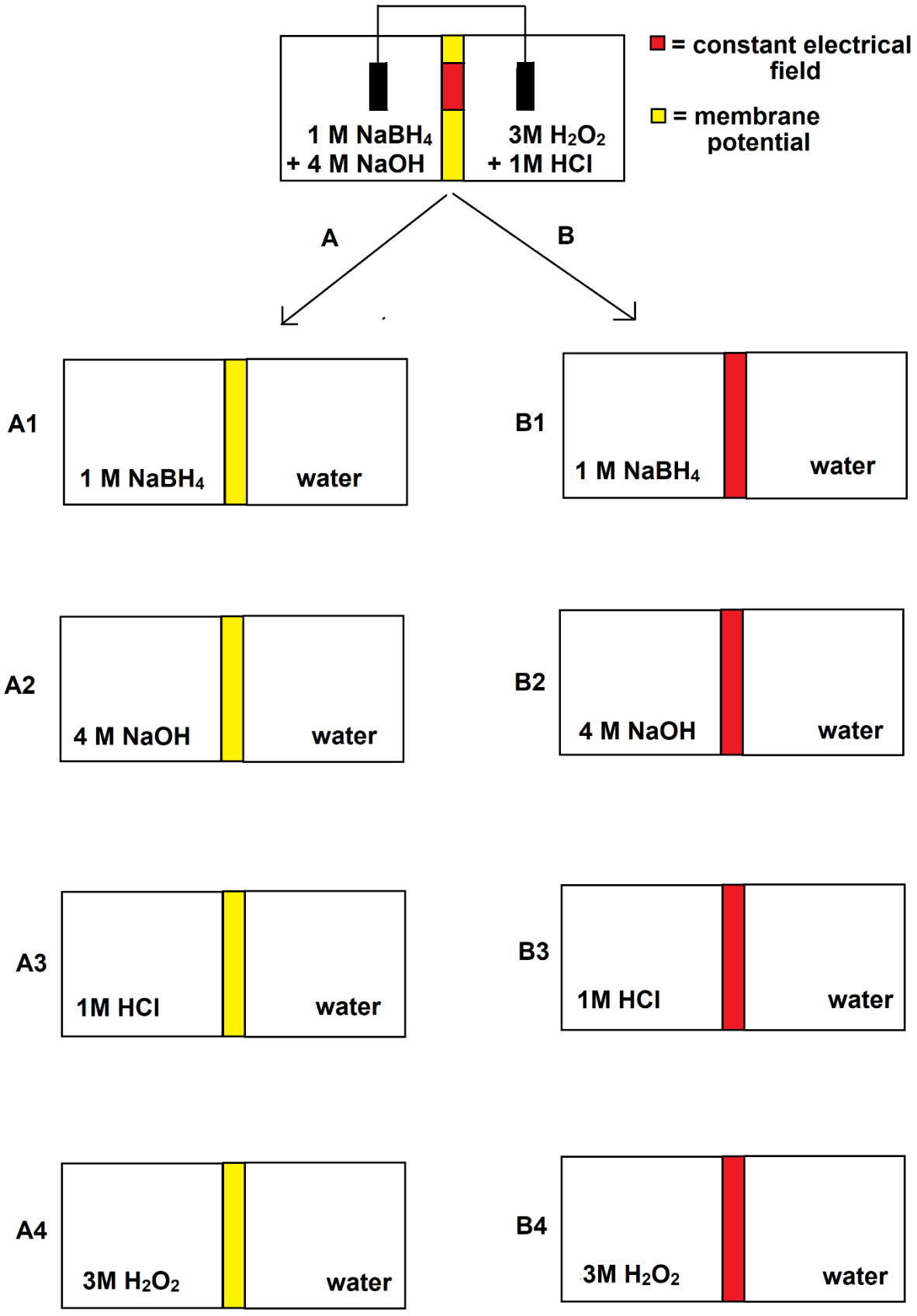

Figure 15 - DBPFC proposed model.

Each compound is dissociated into ions (Eqs. 31-34):

$$NaBH_4 \rightleftharpoons Na^+ + BH_4^- \quad (31)$$

$$NaOH \rightleftharpoons Na^+ + OH^- \quad (32)$$

$$HCl \rightleftharpoons H^+ + Cl^- \quad (33)$$

$$H_2O_2 \rightleftharpoons H^+ + HO_2^- \quad (34)$$

In the case of current equal to zero (A, yellow sections, with membrane potential), the flux can be written as (Eq. 35 and 36):

$$N_i = -D_i^+ \frac{\Delta C_{s,i}}{\Delta x} - C_{s,i} D_i^+ \frac{F}{R*T} \frac{\Delta \Psi_{i,membrane}}{\Delta x} \quad (35)$$

$$N_i = -D_i^- \frac{\Delta C_s}{\Delta x} + C_{s,i} D_i^- \frac{F}{R*T} \frac{\Delta \Psi_i}{\Delta x} \quad (36)$$

So, each sub-system of the yellow sections (Figure 13) could be explicitly written as:

- Sub-system A1 (Eq. 37 and 38)

$$N_{NaBH4} = -D_{Na}^+ \frac{\Delta C_{NaBH4}}{\Delta x} - C_{NaBH4} D_{Na}^+ \frac{F}{R*T} \frac{\Delta \Psi_{NaBH4}}{\Delta x} \quad (37)$$

$$N_{NaBH4} = -D_{BH4}^- \frac{\Delta C_{NaBH4}}{\Delta x} + C_{NaBH4} D_{BH4}^- \frac{F}{R*T} \frac{\Delta \Psi_{NaBH4}}{\Delta x} \quad (38)$$

- Sub-system A2 (Eq. 39 and 40)

$$N_{NaOH} = -D_{Na}^+ \frac{\Delta C_{NaOH}}{\Delta x} - C_{NaOH} D_{Na}^+ \frac{F}{R*T} \frac{\Delta \Psi_{NaOH}}{\Delta x} \quad (39)$$

$$N_{NaOH} = -D_{OH}^- \frac{\Delta C_{NaOH}}{\Delta x} + C_{NaOH} D_{OH}^- \frac{F}{R*T} \frac{\Delta \Psi_{NaOH}}{\Delta x} \quad (40)$$

- Sub-system A3 (Eq. 41 and 42)

$$N_{HCl} = -D_H^+ \frac{\Delta C_{HCl}}{\Delta x} - C_{HCl} D_H^+ \frac{F}{R*T} \frac{\Delta \Psi_{HCl}}{\Delta x} \quad (41)$$

$$N_{HCl} = -D_{Cl}^- \frac{\Delta C_{HCl}}{\Delta x} + C_{HCl} D_{Cl}^- \frac{F}{R*T} \frac{\Delta \Psi_{HCl}}{\Delta x} \quad (42)$$

- Sub-system A4 (Eq. 43 and 44)

$$N_{H2O2} = -D_H^+ \frac{\Delta C_{H2O2}}{\Delta x} - C_{H2O2} D_H^+ \frac{F}{R*T} \frac{\Delta \Psi_{H2O2}}{\Delta x} \quad (43)$$

$$N_{H2O2} = -D_{HO2}^- \frac{\Delta C_{H2O2}}{\Delta x} + C_{H2O2} D_{HO2}^- \frac{F}{R*T} \frac{\Delta \Psi_{H2O2}}{\Delta x} \quad (44)$$

Going from a concentrate solution to a dilute solution, the difference of concentration has a negative sign: in this way, the diffusive term (the first term, referring to the diffusivity parameter) is positive and contributes to the flux N of the molecule.

In the case of a CEM as Nafion (where $D^+ > D^-$), the flux of positive ions is slowed by the membrane potential term (the second term will decrease the first term), while the flux of negative ions is accelerated by the membrane potential term (the second term will be added to the first term).
The total membrane potential (of the whole DBPFC system) is, consequently, the overlayed effect of all sub-systems, according to the superposition principle, and considering the flux direction of the solutions inside the compartments (Eq. 45):

$$\Delta\Psi_{i,membrane} = \Sigma\Delta\Psi_i = \Delta\Psi_{NaBH4} + \Delta\Psi_{NaOH} - \Delta\Psi_{HCl} - \Delta\Psi_{H2O2} \quad (45)$$

In the case of current different to zero (B, red section, with the constant electrical field), the flux can be written as (Eq. 46 and 47),

$$N_i = -D_i^+ \frac{\Delta C_{s,i}}{\Delta x} - C_{s,i} D_i^+ \frac{F}{R*T} E \quad (46)$$

$$N_i = -D_i^- \frac{\Delta C_s}{\Delta x} + C_{s,i} D_i^- \frac{F}{R*T} E \quad (47)$$

where E (Vm^{-1}) is the constant electrical field between the electrodes.

So, each sub-system of the red sections (see figure 15) could be explicitly written as:

- Sub-system B1 (Eq. 48 and 49)

$$N_{NaBH4} = -D_{Na}^+ \frac{\Delta C_{NaBH4}}{\Delta x} - C_{NaBH4} D_{Na}^+ \frac{F}{R*T} E \quad (48)$$

$$N_{NaBH4} = -D_{BH4}^- \frac{\Delta C_{NaBH4}}{\Delta x} + C_{NaBH4} D_{BH4}^- \frac{F}{R*T} E \quad (49)$$

- Sub-system B2 (Eq. 50 and 51)

$$N_{NaOH} = -D_{Na}^+ \frac{\Delta C_{NaOH}}{\Delta x} - C_{NaOH} D_{Na}^+ \frac{F}{R*T} E \quad (50)$$

$$N_{NaOH} = -D_{OH}^- \frac{\Delta C_{NaOH}}{\Delta x} + C_{NaOH} D_{OH}^- \frac{F}{R*T} E \quad (51)$$

- Sub-system B3 (Eq. 52 and 53)

$$N_{HCl} = -D_H^+ \frac{\Delta C_{HCl}}{\Delta x} - C_{HCl} D_H^+ \frac{F}{R*T} E \quad (52)$$

$$N_{HCl} = -D_{Cl}^- \frac{\Delta C_{HCl}}{\Delta x} + C_{HCl} D_{Cl}^- \frac{F}{R*T} E \quad (53)$$

- Sub-system B4 (Eq. 54 and 55)

$$N_{H2O2} = -D_H^+ \frac{\Delta C_{H2O2}}{\Delta x} - C_{H2O2} D_H^+ \frac{F}{R*T} E \quad (54)$$

$$N_{H2O2} = -D_{HO2}^- \frac{\Delta C_{H2O2}}{\Delta x} + C_{H2O2} D_{HO2}^- \frac{F}{R*T} E \quad (55)$$

So, the whole system can be expressed with the overlayed effects of all the sub-systems A1, A2, A3, A4, B1, B2, B3, and B4.

The diffusivity of each molecule (Eq. 56) can be written as:

$$D_s = \frac{(z^+ - z^-) * D^+ * D^-}{z^+ * D^+ - z^- * D^-} \tag{56}$$

So, knowing this model, with a measured flux of ions inside the membrane, an iterative process could be created to obtain the two unknowns of each sub-system, which are the diffusivities of the ions. Knowing the diffusivities of each ion in each membrane, the flux of ions in each type of membrane can be predicted.

2.3.2 Forecast flux with constant initial concentration

The flux of ions through the membrane at a specified time can be predicted, considering the initial concentration in the alkaline solution constant (C_{s0} = constant): so C_{s0} is not a function of time.
So, there is a sample NaOH solution flowing through a membrane to a distilled water solution, in the case of no current (no external electrical field).
If the initial concentration in the acid solution is zero (Eq. 57), C_{s1} can be written as a function of time (Eq. 58):

$$C_{s1}(0)\left[\frac{mol}{cm^3}\right] = 0 \tag{57}$$

$$C_{s1}(t)\left[\frac{mol}{cm^3}\right] = \frac{N\left[\frac{mol}{cm^2{*}s}\right]{*}A_{membrane}[cm^2]{*}t[s]}{V[cm^3]} \tag{58}$$

Initial guess of the positive ion diffusivity inside the membrane D^+ cm^2s^{-1}, and the negative ion diffusivity inside the membrane D^- cm^2s^{-1}, are needed.
The parameter β (Eq. 59) can be written as:

$$\beta\ \left[\frac{V{*}mol}{cm^4}\right] = \frac{R\left[\frac{\mathrm{J}}{\mathrm{mol{*}K}}\right]{*}\mathrm{T[K]}{*}\mathrm{N}\left[\frac{\mathrm{mol}}{cm^2{*}\mathrm{s}}\right]}{2{*}F\left[\frac{C}{mol}\right]} * \left[\frac{D^+\left[\frac{cm^2}{s}\right]-D^-\left[\frac{cm^2}{s}\right]}{D^+\left[\frac{cm^2}{s}\right]{*}D^-\left[\frac{cm^2}{s}\right]}\right] \tag{59}$$

And the membrane potential (Eq. 60) can be written as:

$$\frac{d\Psi(x)}{dx} = \frac{\beta}{C_s(x)} \tag{60}$$

That, considering only the edges of the membrane, can be linearized as (Eq. 61):

$$\frac{\Delta\Psi}{\Delta x} = \frac{\beta}{C_{s1}} \tag{61}$$

This gives a numerical expression of the membrane potential, as a function of time (because it still depends on the ion flux N), shown in Eq. 62 and 63:

$$\Delta\Psi = \frac{\beta{*}\Delta x}{C_{s1}} \tag{62}$$

$$\Delta\Psi = \frac{R{*}\mathrm{T}{*}\mathrm{N}{*}\Delta x}{2{*}F{*}C_{s1}} * \left[\frac{D^+-D^-}{D^+{*}D^-}\right] \tag{63}$$

With the known value C_{s0} (= constant), the difference between concentrations can be written as (Eq. 64):

$$\Delta C_s = C_{s1} - C_{s0} = \frac{N{*}A_{membrane}{*}t}{V} - C_{s0} \tag{64}$$

That is a negative value, because $C_{s0} > C_{s0}$ (since the higher concentration goes to a lower concentration). To balance it, there is the negative sign in front of the diffusion term.
Now, the Nernst-Planck equations are (Eq. 65 and 66):

$$N^+ = -D^+\frac{dC_s(x)}{dx} - C_s(x) * D^+\frac{F}{R{*}T}\frac{d\Psi(x)}{dx} \tag{65}$$

$$N^- = -D^- \frac{dC_s(x)}{dx} + C_s(x) * D^- \frac{F}{R*T} \frac{d\Psi(x)}{dx} \quad (66)$$

And they can be re-written as (Eq. 67 and 68):

$$N^+ = -D^+ \frac{\Delta C_s}{\Delta x} - C_{s1} * D^+ \frac{F}{R*T} \frac{\Delta\Psi(x)}{\Delta x} \quad (67)$$

$$N^- = -D^- \frac{\Delta C_s}{\Delta x} + C_{s1} * D^- \frac{F}{R*T} \frac{\Delta\Psi(x)}{\Delta x} \quad (68)$$

Considering only the positive flux, it can be written as (Eq. 69):

$$N^+ = -D^+ \frac{\left(\frac{N^+ * A_{membrane} * t}{V} - C_{s0}\right)}{\Delta x} - \frac{N^+ * A_{membrane} * t}{V} * \frac{D^+ * F}{R*T*\Delta x} * \frac{R*\mathrm{T}*N^+ * \Delta x}{2*F} * \left[\frac{D^+ - D^-}{D^+ * D^-}\right] * \frac{V}{N^+ * A_{membrane} * t} \quad (69)$$

That can be simplified in Eq. 70:

$$N^+ = -\frac{D^+}{\Delta x} * \left(\frac{N^+ * A_{membrane} * t}{V} - C_{s0}\right) - \frac{N^+ * D^+}{2} * \left[\frac{D^+ - D^-}{D^+ * D^-}\right] \quad (70)$$

The correlated explicit equation is shown in Eq. 71:

$$0 = -N^+ - \frac{D^+}{\Delta x} * \left(\frac{N^+ * A_{membrane} * t}{V} - C_{s0}\right) - \frac{N^+ * D^+}{2} * \left[\frac{D^+ - D^-}{D^+ * D^-}\right] \quad (71)$$

And gather the known N^+, the Eq. 72 is obtained:

$$0 = -N^+ * \left[1 + \left(\frac{D^+ * A_{membrane} * t}{\Delta x * V}\right) + \frac{D^+}{2} * \left[\frac{D^+ - D^-}{D^+ * D^-}\right]\right] + \frac{D^+ * C_{s0}}{\Delta x} \quad (72)$$

The same process is valid also for the negative flux N^- (Eq. 73), paying attention to the signs:

$$0 = -N^- * \left[1 + \left(\frac{D^- * A_{membrane} * t}{\Delta x * V}\right) - \frac{D^-}{2} * \left[\frac{D^+ - D^-}{D^+ * D^-}\right]\right] + \frac{D^- * C_{s0}}{\Delta x} \quad (73)$$

It is good to remark that this is possible only if considering a constant concentration in the alkaline solution (when C_{s0} = constant), so C_{s0} is not a function of time, neither a function of the flux.
In the case of C_{s0} = f(t), so C_{s0} = f(N), they should have been gathered with all the other terms depending on N: in this case the only values that will let having a zero in the equation will be the extreme values of t=0, N=0, D^+=0 or D^-=0, not useful to discover.
Returning to the linearization, new parameters K1 (Eq. 74), L1 (Eq. 75), K2 (Eq. 76) and L2 (Eq. 77) can be introduced:

$$K1 = \frac{D^+ * A_{membrane} * t}{\Delta x * V} \quad (74)$$

$$L1 = \frac{D^+}{2} * \left[\frac{D^+ - D^-}{D^+ * D^-}\right] \quad (75)$$

$$K2 = \frac{D^- * A_{membrane} * t}{\Delta x * V} \quad (76)$$

$$L2 = \frac{D^-}{2} * \left[\frac{D^+ - D^-}{D^+ * D^-}\right] \quad (77)$$

To have the final equations (for zero current), written in Eq. 78 and 79:

$$N^+ = \frac{D^+ * C_{s0}}{\Delta x} * \frac{1}{[1 + K1 + L1]} \quad (78)$$

$$N^- = \frac{D^- * C_{s0}}{\Delta x} * \frac{1}{[1 + K2 - L2]} \quad (79)$$

Seeing that there is electroneutrality in the solutions, it is still valid the correlation $N^+=N^-=N$.
These formulas are set on an Excel file, to easily find the flux knowing the time t and the constant initial concentration C_{s0}.
The calculation can be repeated for each separate solution involved, paying attention to the sign and to the directions of the flow, to obtain the whole flux in case of zero current (no external electrical field)

In the case of electrical current (where there is an external electrical field E), with E Vcm^{-1}, the Nernst-Planck equations can be written as (Eq. 80 and 81):

$$N^+ = -D^+ \frac{\Delta C_s}{\Delta x} - C_{s1} * D^+ \frac{F*E}{R*T} \tag{80}$$

$$N^- = -D^- \frac{\Delta C_s}{\Delta x} + C_{s1} * D^- \frac{F*E}{R*T} \tag{81}$$

Where the positive flux can be re-written as (Eq. 82):

$$N^+ = -D^+ \frac{\left(\frac{N^+ * A_{membrane} * t}{V} - C_{s0}\right)}{\Delta x} - \frac{N^+ * A_{membrane} * t}{V} * \frac{D^+ * F * E}{R*T} \tag{82}$$

An explicit equation is found (Eq. 83):

$$0 = -N^+ - \frac{D^+}{\Delta x} * \left(\frac{N^+ * A_{membrane} * t}{V} - C_{s0}\right) - \frac{N^+ * A_{membrane} * t}{V} * \frac{D^+ * F * E}{R*T} \tag{83}$$

And the unknown N^+ can be gathered in Eq. 84:

$$0 = -N^+ * \left[1 + \left(\frac{D^+ * A_{membrane} * t}{\Delta x * V}\right) + \frac{A_{membrane} * t * D^+ * F * E}{V * R * T}\right] + \frac{D^+ * C_{s0}}{\Delta x} \tag{84}$$

The same can be done also for the negative flux N^- (Eq. 85), paying attention to the signs:

$$0 = -N^- * \left[1 + \left(\frac{D^- * A_{membrane} * t}{\Delta x * V}\right) - \frac{A_{membrane} * t * D^- * F * E}{V * R * T}\right] + \frac{D^- * C_{s0}}{\Delta x} \tag{85}$$

New parameters can be introduced, as V1 (Eq. 86), W1 (Eq. 87), V2 (Eq. 88), W2 (Eq. 89):

$$V1 = \frac{D^+ * A_{membrane} * t}{\Delta x * V} \tag{86}$$

$$W1 = \frac{A_{membrane} * t * D^+ * F * E}{V * R * T} \tag{87}$$

$$V2 = \frac{D^- * A_{membrane} * t}{\Delta x * V} \tag{88}$$

$$W2 = \frac{A_{membrane} * t * D^- * F * E}{V * R * T} \tag{89}$$

(It is supposed to be K1≠ V1, and K2≠ V2 because they have a different membrane area)

To have the final equations (with a constant external electrical field) as shown in Eq. 90 and 91:

$$N^+ = \frac{D^+ * C_{s0}}{\Delta x} * \frac{1}{[1+V1+W1]} \tag{90}$$

$$N^- = \frac{D^- * C_{s0}}{\Delta x} * \frac{1}{[1+V2-W2]} \tag{91}$$

So, resuming, assuming C_{s0} = constant, selecting a time, guessing the positive ion diffusivity inside the membrane D^+ cm^2s^{-1}, and the negative ion diffusivity inside the membrane D^- cm^2s^{-1}, a predicted flux can be obtained just combining the equations with and without current.

2.3.3 Concentration profile and membrane potential profile inside the membrane

Also, a concentration profile $C_s(x)$ and the membrane potential profile $\Delta\Psi(x)$ inside the membrane can be found.

To do it, an average measured stabilized flux N mol*cm^{-2} s^{-1} must be assumed, and a time selected: in this way, there is the concentration C_{s0} as a function of time (just in case there is no recirculation/make-up flow), as shown in Eq. 92:

$$C_{s0}(t) = C_{s0} - \frac{N*A_{membrane}*t}{V} \quad (92)$$

The positive ion diffusivity inside the membrane D^+ cm^{2}s^{-1}, and the negative ion diffusivity inside the membrane D^- cm^{2}s^{-1}, should be guessed as an initial hypothesis.

The salt concentration can be expressed as in Eq. 93 and 94:

$$\frac{dC_s(x)}{dx} = -A \quad (93)$$

$$C_s(x) = C_{s0} - A * x \quad (94)$$

With the definition of the parameter A (Eq. 95):

$$A = \frac{N*(D^- + D^+)}{2*D^+*D^-} \quad (95)$$

The value "A" is critical, because A*Δx must be always less than C_{s0}, otherwise matter would have been created.

A presence of positive ions inside the membrane is considered (for example a concentration of 1000 molm^{-3} of H^+ inside the Nafion membrane, with a density of 1 kg m^{-3}), to have a difference between the concentration of positive and negative ions inside.

So, for the selected time, the concentrations can be plotted inside the membrane thickness (figure 14).

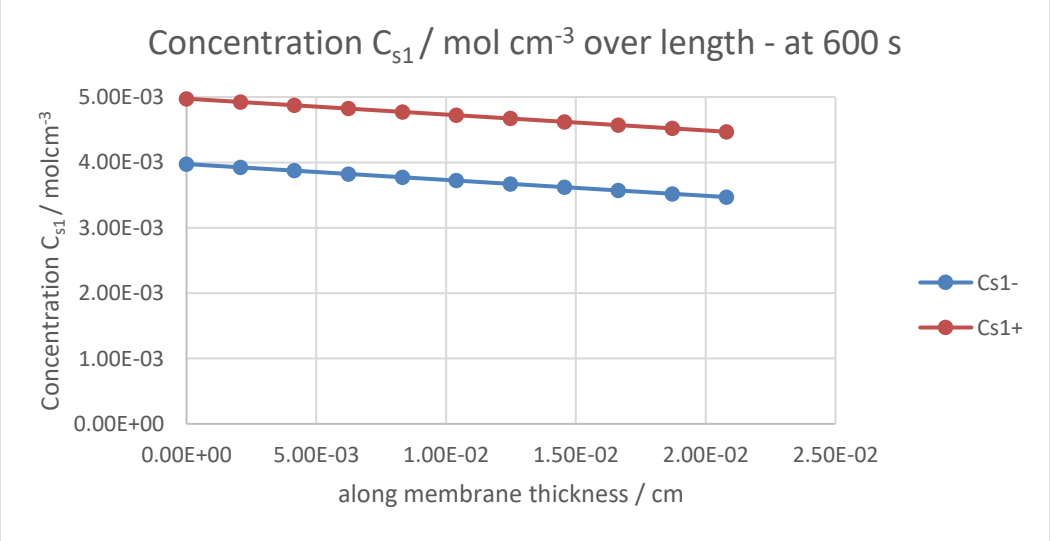

Figure 16 - Example of concentration profile with an average flux of 1.08E-07 mol s^{-1} cm^{-2}, a positive diffusivity D^+ = 5E-6 cm^2 s^{-1}, and a negative diffusivity D^- = 4E-6 cm^2 s^{-1}, at 600 seconds.

Meanwhile, the membrane potential can be written as Eq. 96:

$$\Psi(x) = \Psi_0 + \frac{\beta}{A} * \left[\ln\left(\frac{C_{s0}}{C_{s0} - A*x}\right)\right] \quad (96)$$

With the definition of the parameter β (Eq. 97):

$$\beta \left[\frac{V*mol}{cm^4}\right] = \frac{R\left[\frac{J}{mol*K}\right]*T[K]*N\left[\frac{mol}{cm^2*s}\right]}{2*F\left[\frac{C}{mol}\right]} * \left[\frac{D^+\left[\frac{cm^2}{s}\right] - D^-\left[\frac{cm^2}{s}\right]}{D^+\left[\frac{cm^2}{s}\right] * D^-\left[\frac{cm^2}{s}\right]}\right] \quad (97)$$

Assuming $\Psi_0 = 0$, the membrane potential profile can be plotted inside the membrane thickness, at the specified time (figure 15):

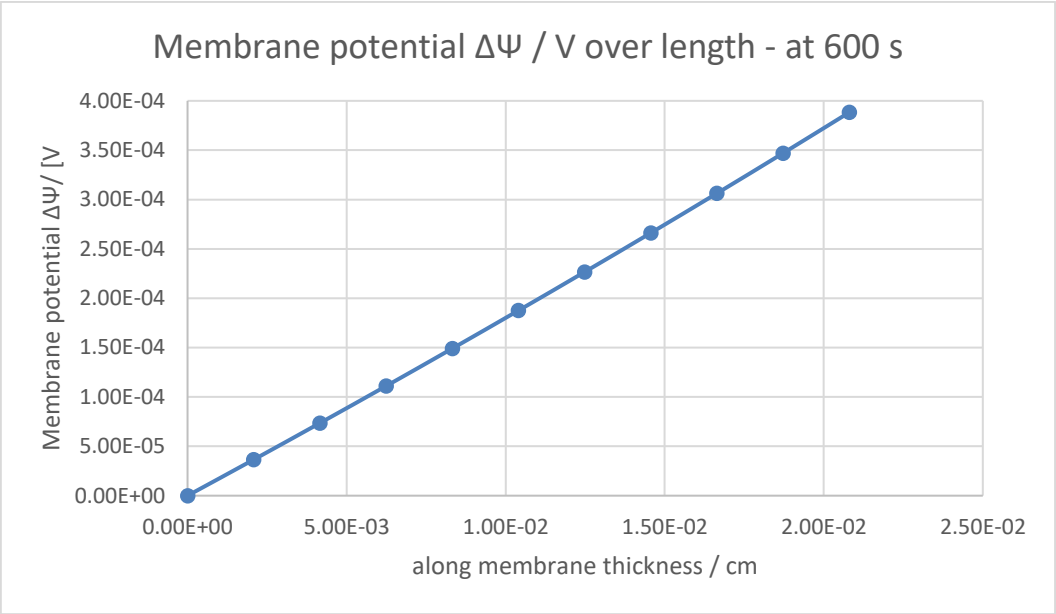

Figure 17 - Example of membrane potential profile with an average flux of 1.08E-07 mol s^{-1} cm^{-2}, a positive diffusivity D^+ =5E-6 cm^2 s^{-1}, and a negative diffusivity D^- =4E-6 cm^2 s^{-1}, at 600 seconds.

The weak point of this method is that, with the same starting point of our DBPFC model, so an initial concentration of 0.004 mol cm^{-3} and a volume of 75 cm^3, there must be a limitation on the guessing of diffusivities, otherwise the term A*Δx is not anymore less than C_{s0}. (Eqs. 98-100)

$$C_{s0} > A * \Delta x \quad (98)$$

$$C_{s0} > \frac{\Delta x*N*(D^- + D^+)}{2*D^+*D^-} \quad (99)$$

$$N < \frac{2*C_{s0}*D^+*D^-}{\Delta x*(D^- + D^+)} \quad (100)$$

This is due to the fact that an average stabilized measured flux N is assumed, but in reality, also the flux N will change during time (so, as seen in the experiment).

Chapter 3

Results and Discussion

3.1 NaOH-Nafion experiment

To validate the proposed model, an example of a sub-system of the DBPFC is taken, to show experimentally that the ions from a 4 M NaOH solution will pass through a Nafion membrane, increasing the pH of the second compartment containing only distilled water. Therefore, not only Na^+ will be transferred inside the Nafion CEM, but also OH^- will pass to maintain the electroneutrality of the solutions. As the Na^+ ions will pass at the same velocity of OH^-, there will be a delayed Na^+ passage through the membrane due to the OH^- hindering.

All the Nafion membranes were already pre-activated, replacing H^+ inside with Na^+. Moreover, the same concentrations of the real DBPFC are used, but no electrodes are used, so no electro-components were used for the experiments.

The pH probe was calibrated before the experiments, with the references of pH=7.00, pH=4.01, and pH=10.00 (Figure 18). The references should be at 25 °C, so there could be a little difference due to the temperature difference.

Figure 18 – Standards used for pH calibration.

Unlucky, with the reference of pH=12.00 the results could have been better, but it was not possible to do. This led to an “Out of range” error above measured pH of 12.00, and an additional “Electrode out of species” error above pH= 13.00: so, in the measurements above 12.00 the error of the measured pH is not known exactly, so there could be some little differences with the real values in the solutions.

11 tests (with the same concentration) were made, with 3 different membranes:

- Nafion N117 #1
- Nafion N117 #2
- Nafion N117 #4

Here a resume of the tests:

- Test 1, Nafion N117 #1

- Test 2, Nafion N117 #1
- Test 3, Nafion N117 #2
- Test 4, Nafion N117 #1
- Test 5, Nafion N117 #2
- Test 6, Nafion N117 #4
- Test 7, Nafion N117 #1
- Test 8, Nafion N117 #2
- Test 9, Nafion N117 #4
- Test 10, Nafion N117 #1
- Test 11, Nafion N117 #1

It was not possible to obtain the distilled water at exactly pH=7.00, because distilled water is more reactive than tap water and it easily reacts with CO_2 present in the air. So, before the experiment, 75 cm^3 of distilled water were continuously moved (with a vibration system under the cell) till having a pH of 5.95 at T = 23,5 °C. Then it was poured into one compartment of the cell, while 75 cm^3 of NaOH solution (4 M of NaOH = 0.004 mol cm^{-3}) was poured in the other side, with some parafilm on the top holes of the fuel cell (to avoid/hindering the formation of CO_3^-). Then the pH probe is inserted, to start measuring the pH in the water compartment. In the first tests, a movement tool was positioned under the cell, to have more homogeneous solutions inside. The pH was measured every 5 minutes.

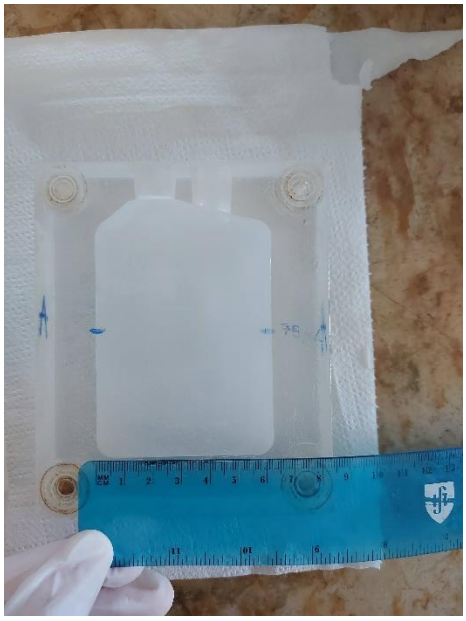

Figure 19 - Active membrane width = 6,5 cm.

Figure 20 - Active membrane height = 4,5 cm.

The volume inside will not fill the whole compartment, because some space on the top is left for the gas production. So, the active membrane of the experiment is calculated as height*width = 4.5*6.5= 29.25 cm^2 (Figure 19 and 20).

After 4 hours of experiment, after all the night without movement (after 18 hours and 20 minutes from the start of the experiment), the measured pH was pH=13.84 at T = 23,1 °C. This long experiment

corroded the rubber part to avoid leakage (also colouring the solutions, with the brown colour of the rubber parts), so the following test were performed in a shorter time period (around 1 hour).

A very big increase of pH in the first minutes was spotted (while a much slower passage of OH^- in the distilled water compartment was expected): the membrane could be not washed correctly before using it. So, for the second experiment, the same experiment was repeated with the same membrane, but letting it sink 40 min in millipore water (distilled water).

In test 2, the pH was measured each minute, while the distilled water used was at the beginning at pH=6-06 at T = 23,5 °C.

In test 3, the test was repeated with a second membrane (different from the first one), measuring the pH every 30 seconds, and with an initial distilled water in the range of pH= 5.95-6.07 at T = 23,5 °C

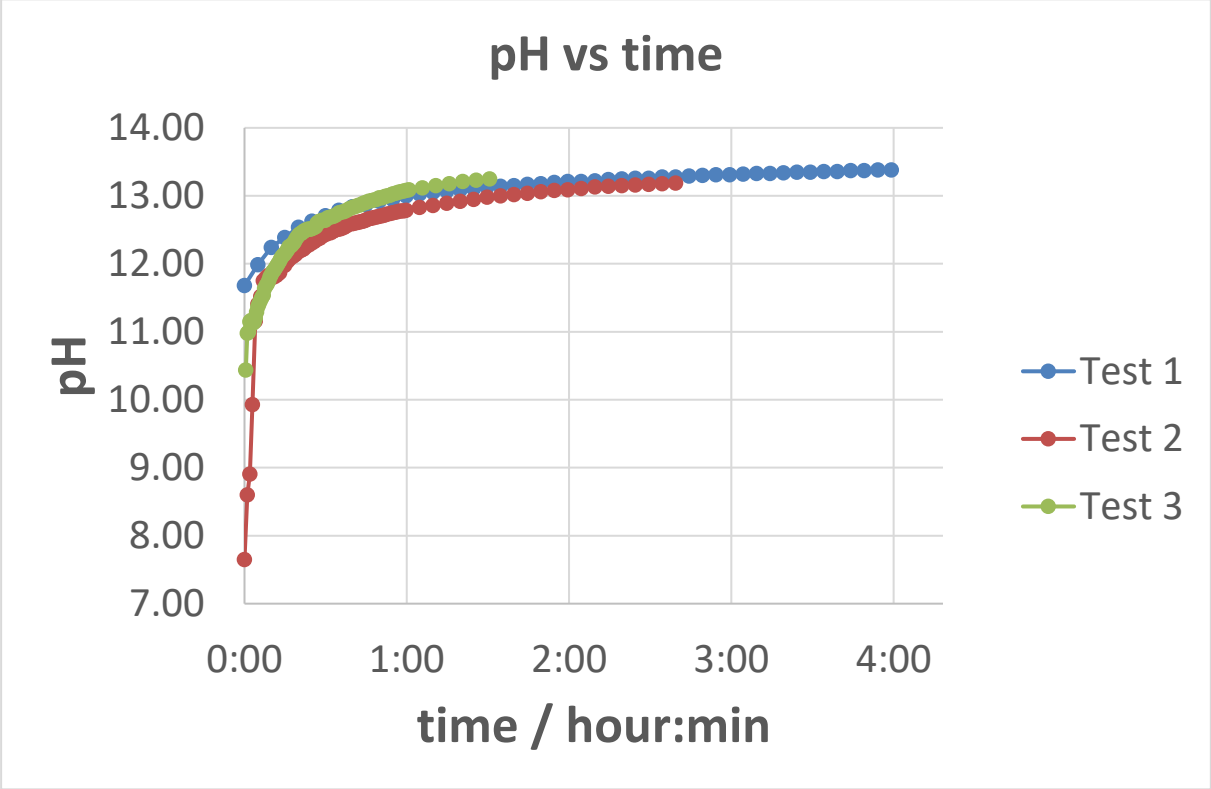

Figure 21 - Tests 1, 2, and 3. 4M NaOH passing through Nafion N117. Measurements of the Millipore water pH with time. Experiments done in triplicate.

From Figure 21, it is shown that long experiments will lead anyway to a continuous increase of pH, so from the fourth experiment only shorter tests were performed, but measuring the pH in shorter time steps.

In test 4, the experiment was repeated with membrane number 1, but this time trying to stabilize the distilled water inside before starting the experiment: the distilled water was left inside the cell for 10 minutes of stabilization at PH = 9.94, with the temperature in the range 22.4-22.6 °C. From this test and so on, the pH in the experiments was recorded and noted at each second after the starting of the experiment.

In test 5, the distilled water inside the cell was stabilized only for 30 s at pH = 10,17, with the temperature T = 23.7 °C

In test 6, a third membrane was used, with the distilled water stabilized inside the cell for 30 s at pH = 10.58, with the temperature T = 24.4 °C.

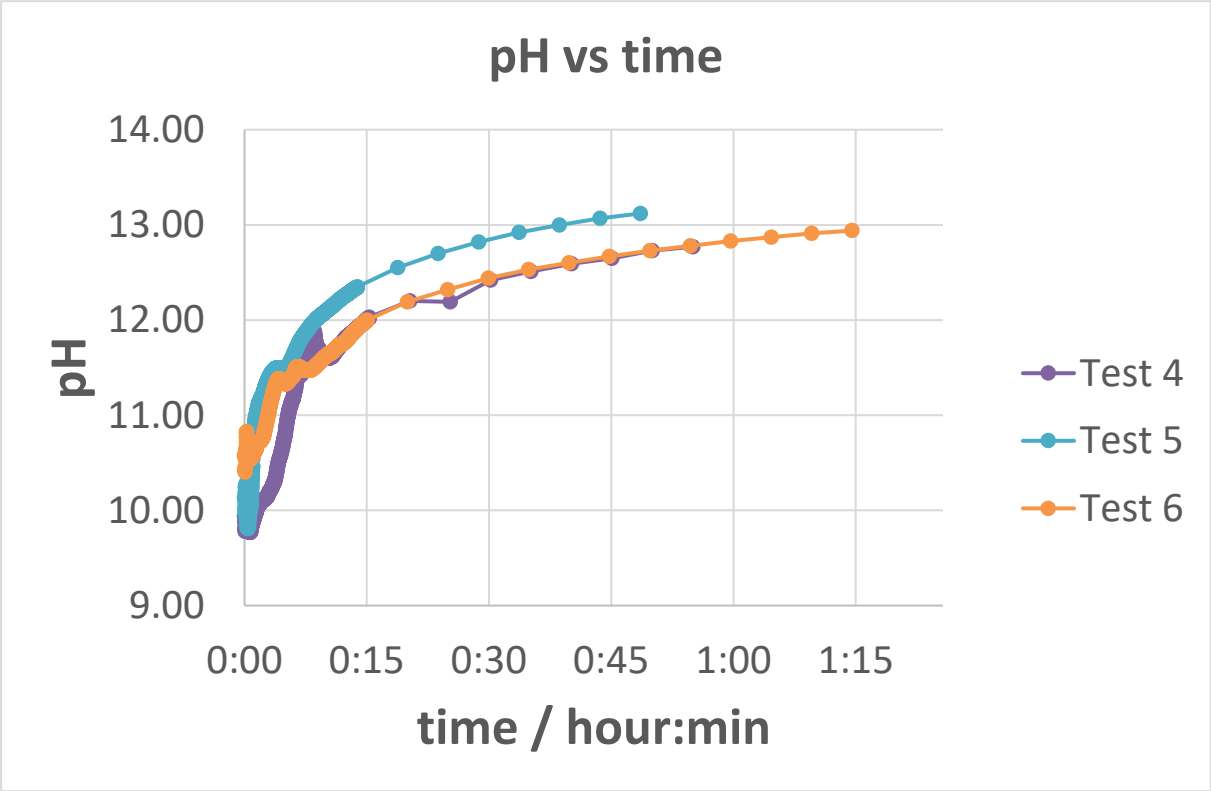

Figure 22 - Tests 4, 5, and 6. 4M NaOH passing through Nafion N117. Measurements of the Millipore water pH with time. Experiments done in triplicate

In Figure 22, a lot of variation is still visible in the first minutes. To be sure that the increase of pH was only the consequence of the OH- passage between the compartments, the tests were performed again with the three membranes using nitrogen bubbling, to have a saturation of nitrogen in both solutions (this minimizes the concentration polarization close to the membrane): these were the only change for the test 7, 8 and 9.

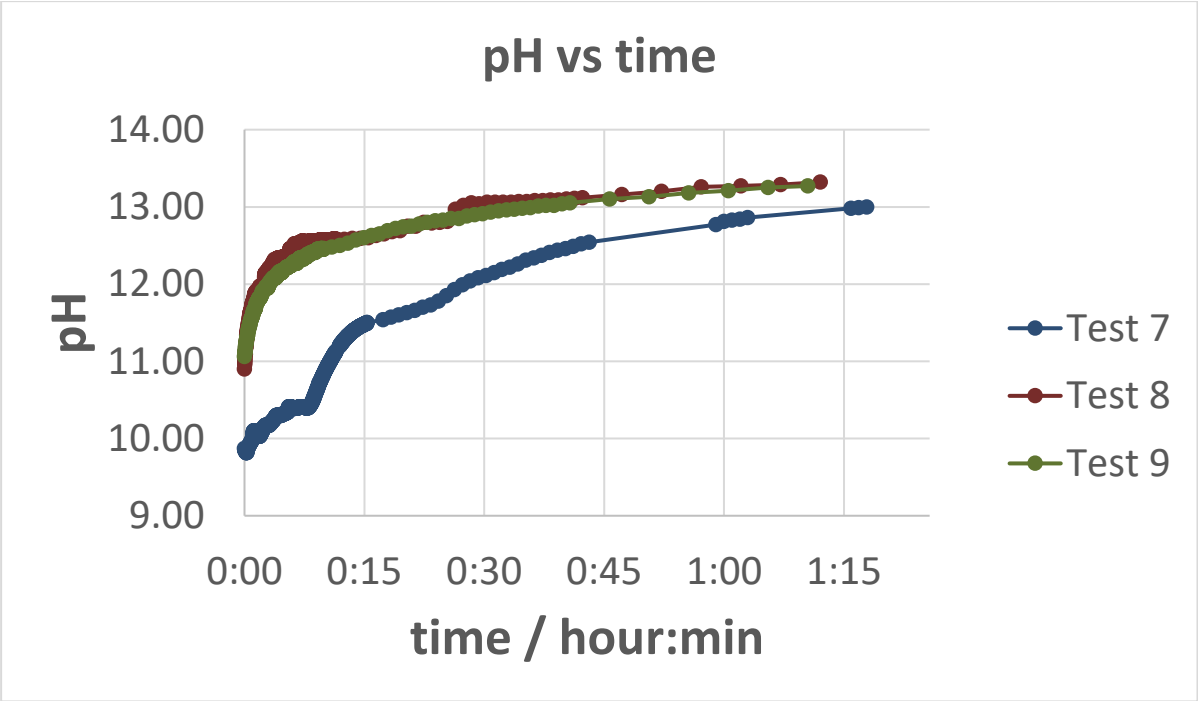

Figure 23 - Tests 7, 8, and 9. 4M NaOH passing through Nafion N117. Measurements of the Millipore water pH with time. Experiments done in triplicate.

In Figure 23, an overlapping of the results is still not visible, so other two tests were performed (test 10 and 11), with the same membrane number 1, but trying to stabilize the pH of the distilled water with nitrogen bubbling for a longer time before the experiments.

In test 10, there was a rough stabilization of distilled water with nitrogen bubbling for 30 minutes in the range 10.00<pH<10.07.

In test 11, there was a rough stabilization of distilled water with nitrogen bubbling for 30 minutes in the range 10.91<pH<11.01.

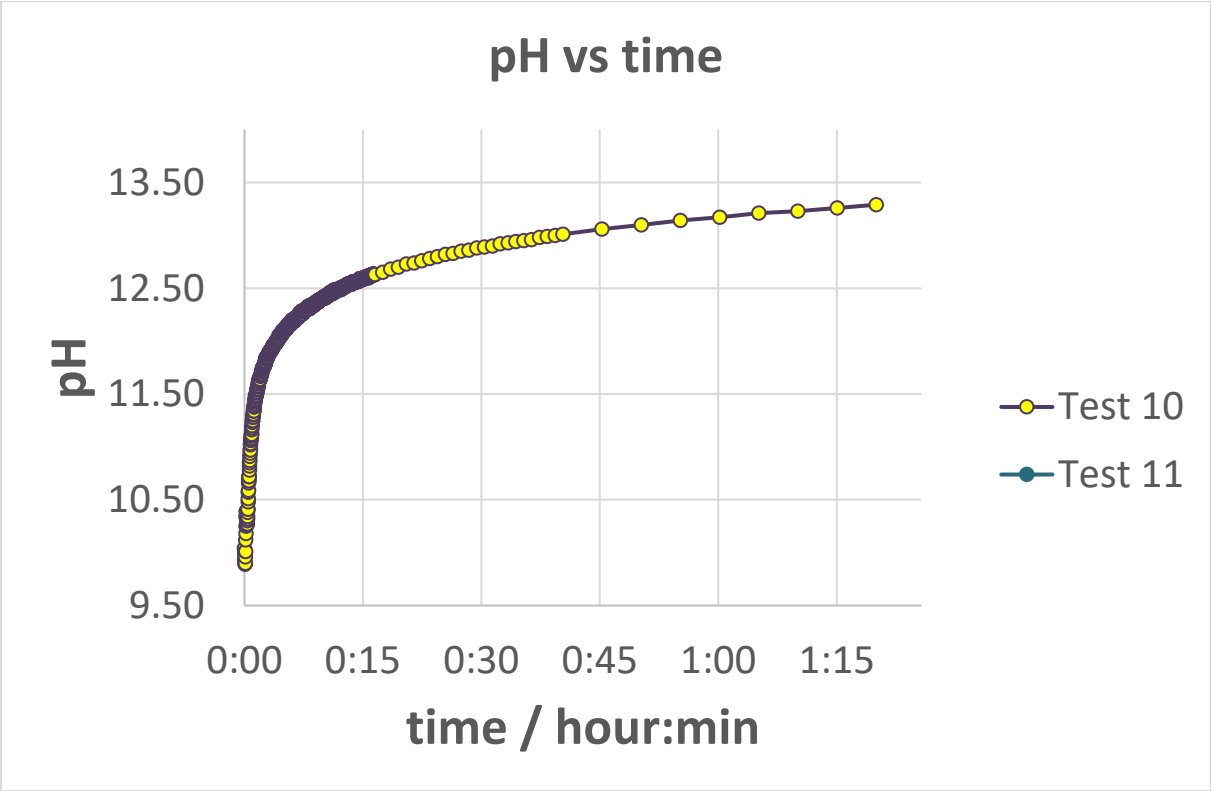

Figure 24 - Tests 10 and 11. 4M NaOH passing through Nafion N117. Measurements of the Millipore water pH with time. Experiments done in duplicate

From figure 24, an overlapping in tests 10 and 11 are shown. If one compartment is empty, the solution will not pass through the membrane (also because the membrane was not cracked or broken): this is an additional validation, where the solution will pass through the membrane only as dissociated ions, and not as a molecule.

3.2 NaOH-Nafion data analysis

From the excel data with all tests, the pH-comparison (figure 25) and OH^- passing (Figure 26) among all the membranes could be shown.

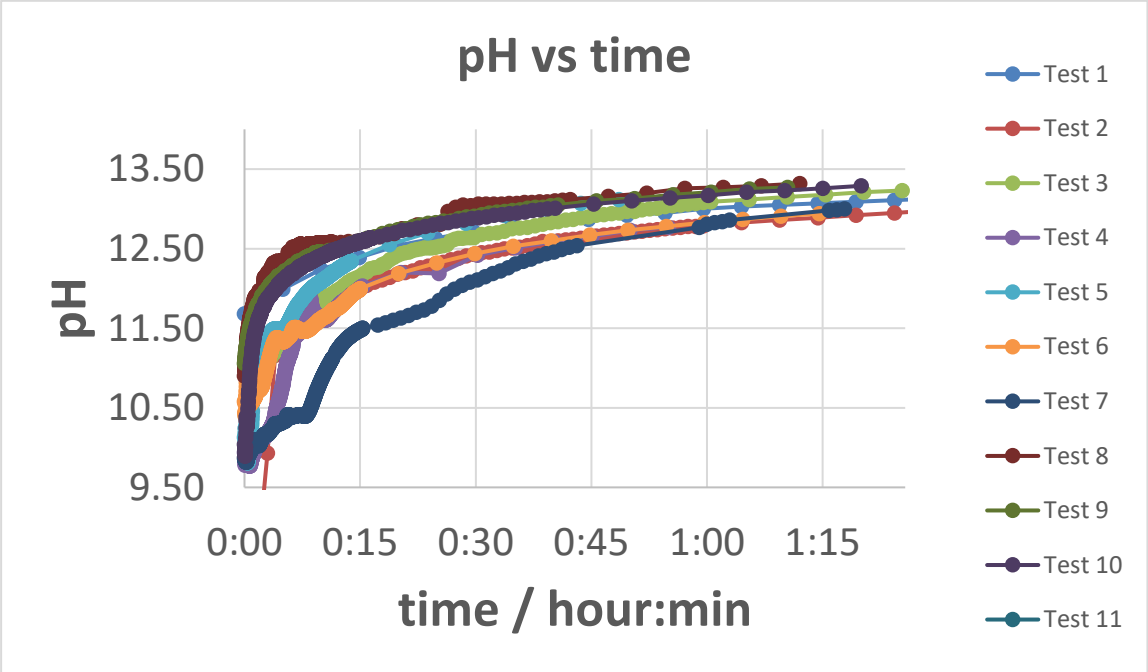

Figure 25 - pH comparison among all tests. 4M NaOH passing through Nafion N117. Measurements of the Millipore water pH with time

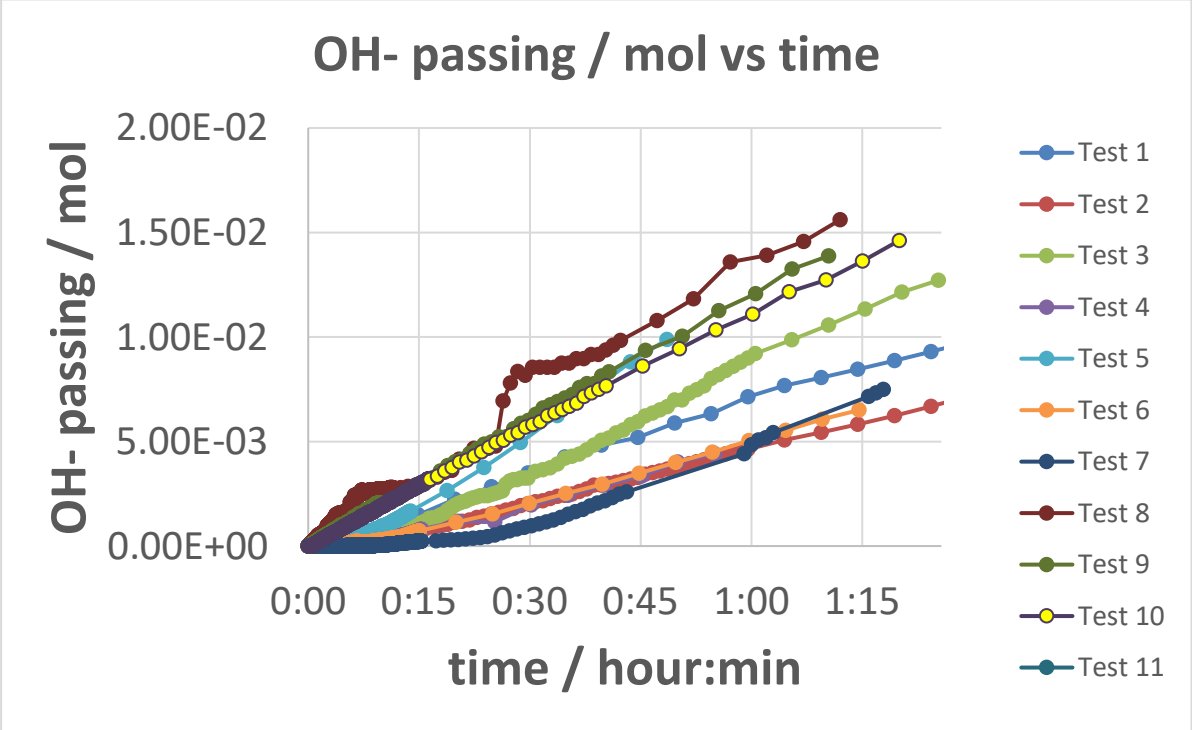

Figure 26 - Comparison of OH^- moles passing, among all tests. 4M NaOH passing through Nafion N117. Measurements of the Millipore water pH with time.

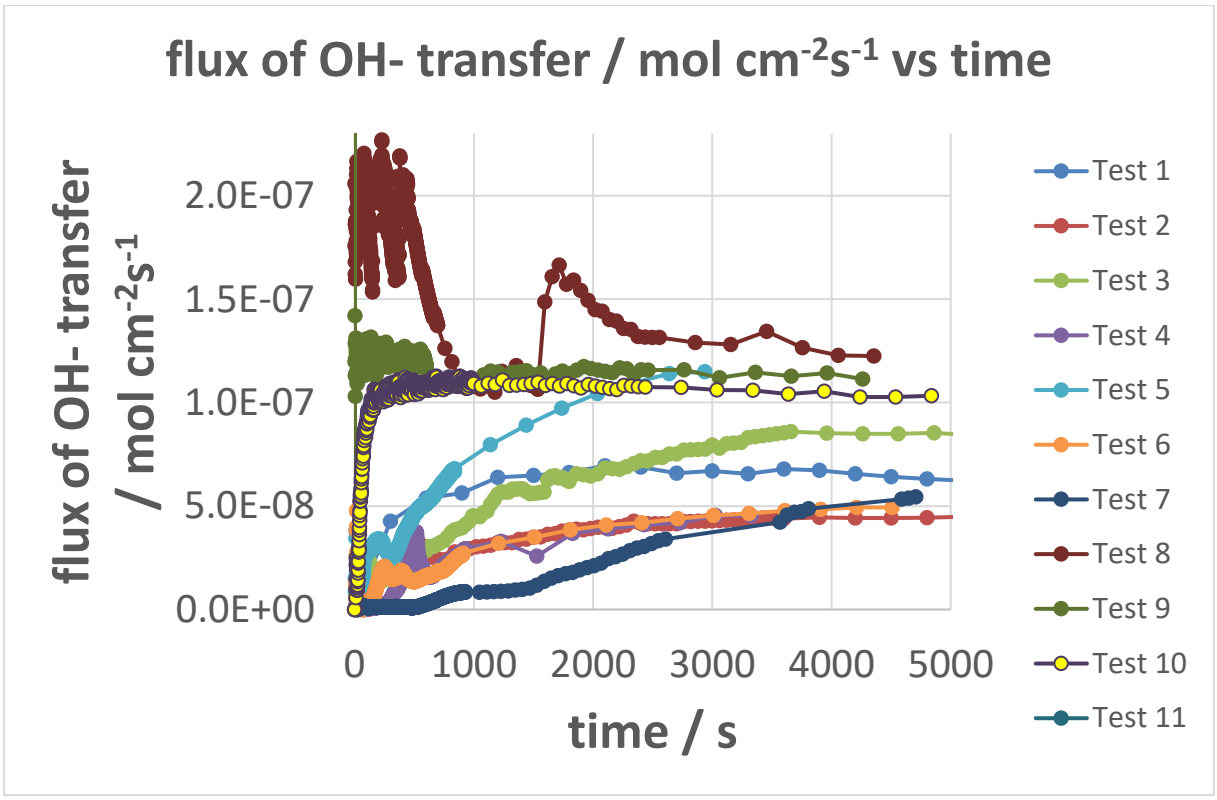

Figure 27 - Comparison of OH^- flux, among all tests. 4M NaOH passing through Nafion N117. Measurements of the Millipore water pH with time.

In Figure 27, it could be more interesting to highlight the trends of the last two tests (test 10 and 11), where with the nitrogen bubbling and the stabilization of the solutions (referred to the time spent before the experiment to have constant pH value in the Millipore water, to start with a roughly stable pH value of reference), the values of OH- passing and OH- flux were more precise as possible.

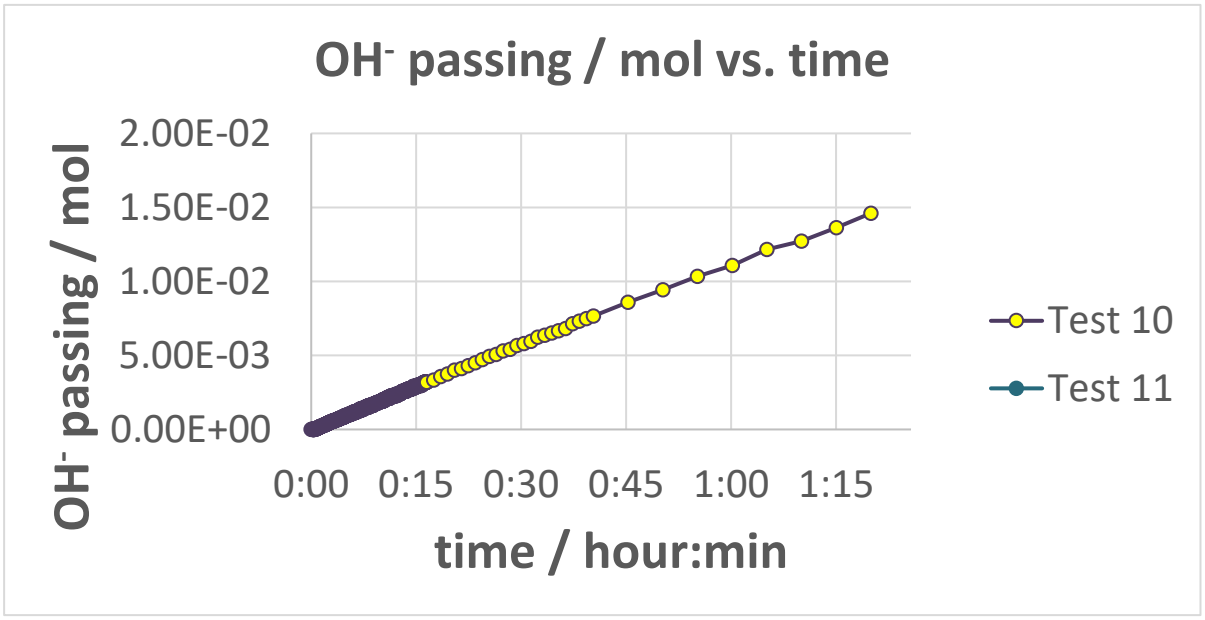

Figure 28 - OH^- moles passing with time, in tests 10 and 11

In Figure 28, it's possible to see the OH^- moles passing with time. In both duplicated experiments, the OH^- moles are increased in a linear way, so with a constant increasing slide, that could be easily extrapolated with a first-order linear equation with angular coefficient.

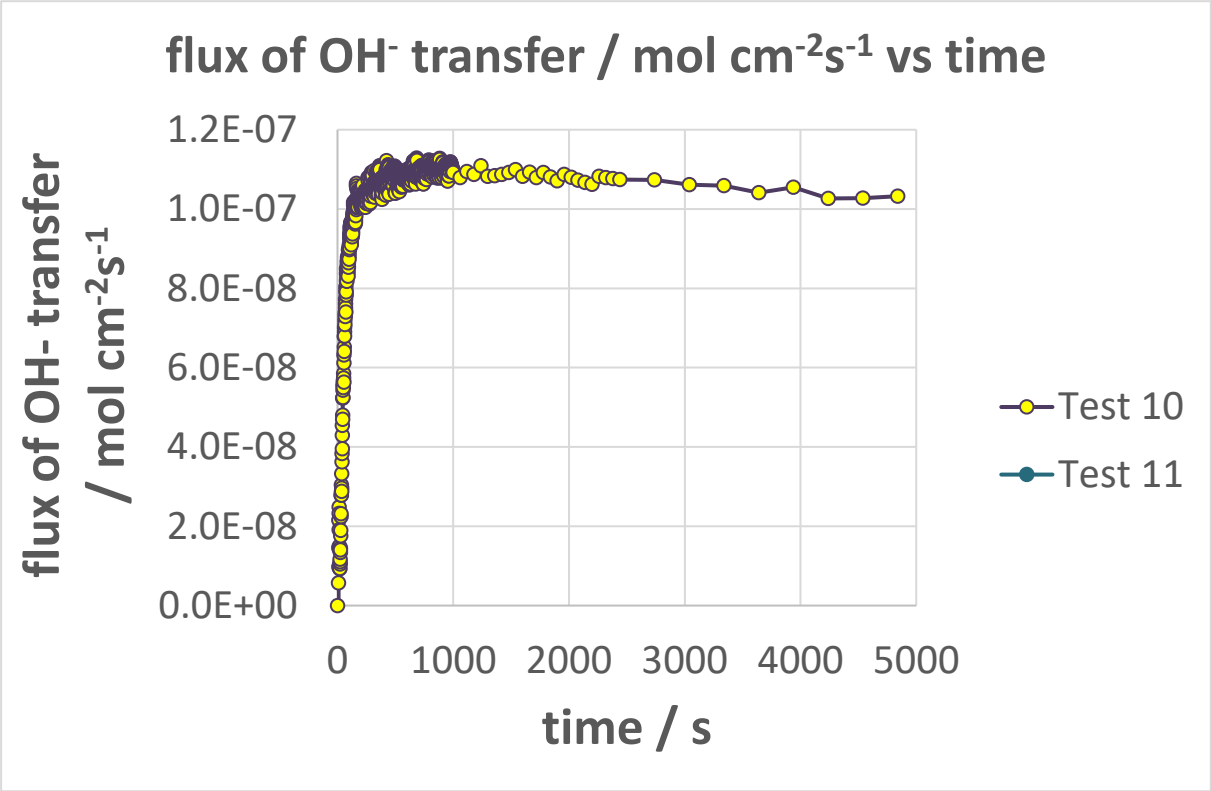

Figure 29 - OH^- flux with time, in tests 10 and 11

In Figure 29, the flux of OH^- is showed. For this graph is considered the effective seconds passed from the start of the experiment, and then it is compared to the active membrane area used in the experiment. It has some delayed of time, because in the first seconds recorded, the flux gives a not-possible negative value (probably due to the rapid change in the pH measurement. So, if Figure 28 shows how an increased moles of OH^- has passed to the other side of the membrane at a selected time, Figure 29 shows how (after the first seconds) the same amount of moles passes in the membrane section for each second: this means that, while inside the membrane there are always the same amount of OH^- transferring, in the second compartment of the cell the OH^- are increasing (starting from zero, seeing that in the second compartment there is initially only Millipore water).

In addition, in the majority of the tests, it is possible to spot this kind of stabilization with time.

3.3 Diffusivities finder – Python code

With a code created in Python, considering the electroneutrality of the solutions (Donnan's equilibrium), it is possible to iterate step by step, to compare the ions flux, and obtain the diffusivities of the ions in the membranes. For computations that are not very long and CPU intensive, Python is an excellent tool.

The values of temperature, flux, C_{s1}, and ΔC, were used to feed the code, and to get as results the two different diffusivities of Na^+ and OH^- (for each test). For the last experiments with thousands of lines of data, only 600 lines were considered to lower the computational cost. The code is shown in Annex B.

Test 1

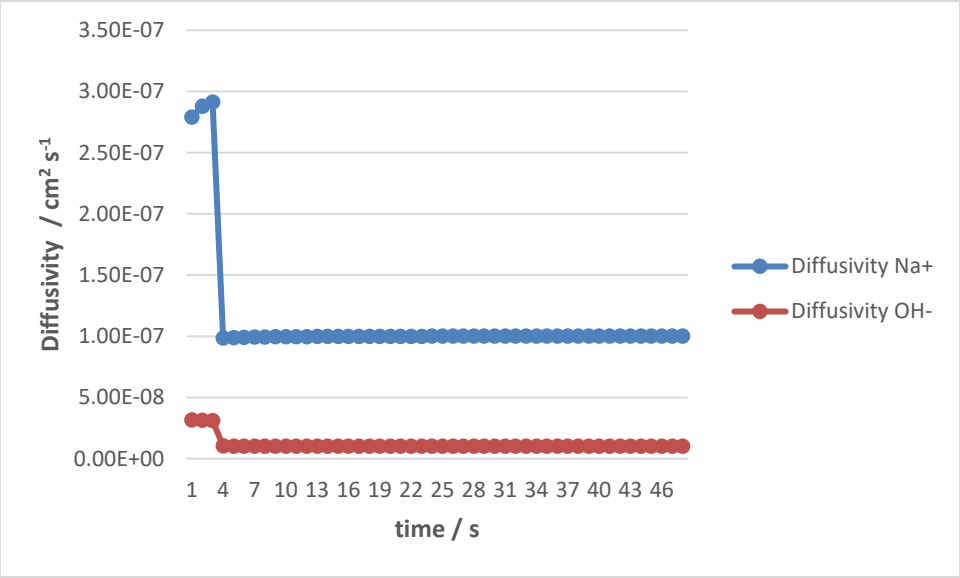

Figure 30 - Test 1, diffusivities values using a diffusivities finder in Python code.

From Figure 30, values stabilized are stabilized at:

D_{Na+} [cm^2/s] = 1.00E-07

D_{OH-} [cm^2/s] = 1.02E-08

Test 2

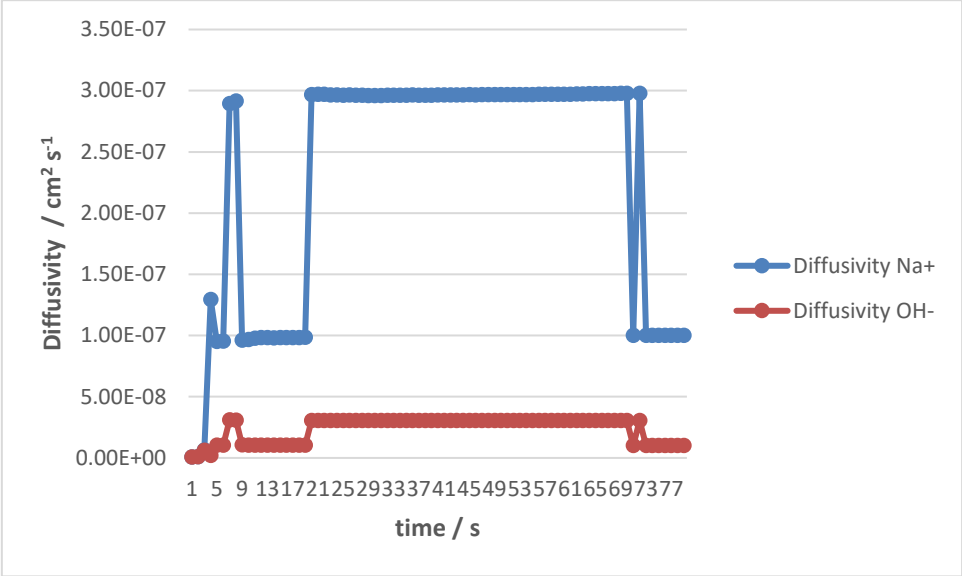

Figure 31 - Test 2, diffusivities values using a diffusivities finder in Python code.

From Figure 31, the final vales are (not-stabilized) at:

D_{Na+} [cm^2/s] = 1.00E-07

D_{OH-} [cm^2/s] = 1.02E-08

Test 3

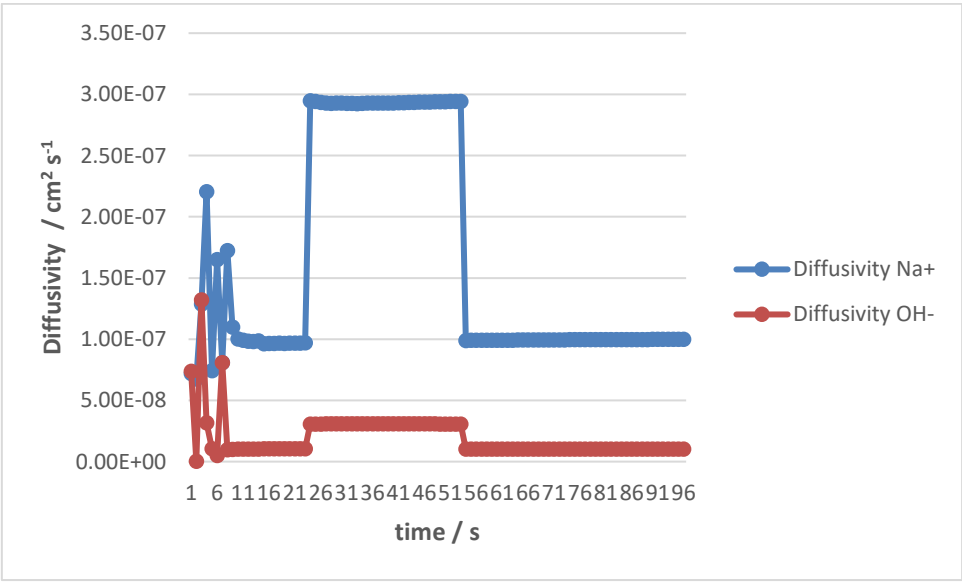

Figure 32 - Test 3, diffusivities values using a diffusivities finder in Python code.

From Figure 32, values are stabilized at:

D_{Na+} [cm^2/s] = 1.00E-07

D_{OH-} [cm^2/s] = 1.02E-08

Test 4

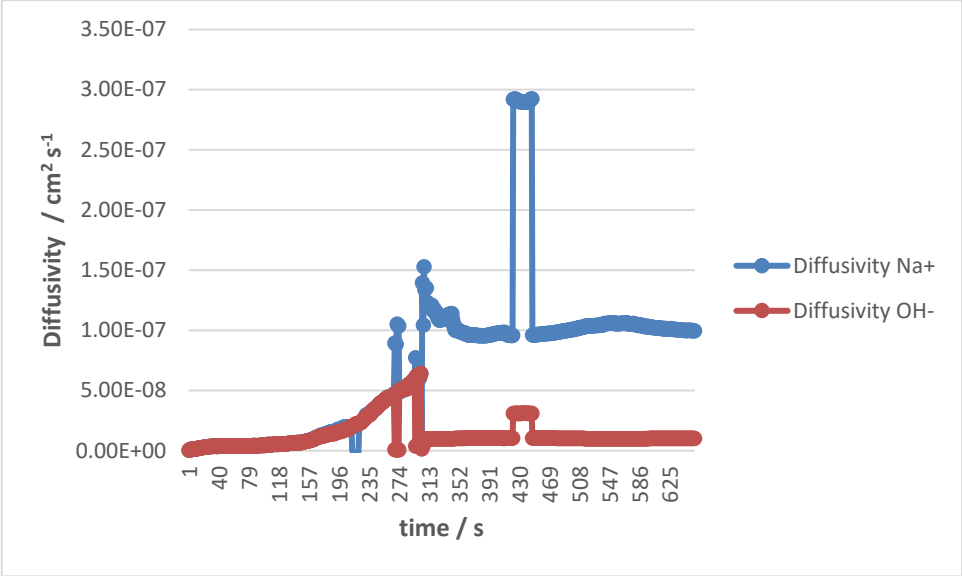

Figure 33 - Test 4, diffusivities values using a diffusivities finder in Python code.

From Figure 33, values are stabilized at:

D_{Na+} [cm²/s] = 9.95E-08

D_{OH-} [cm²/s] = 1.02E-08

Test 5

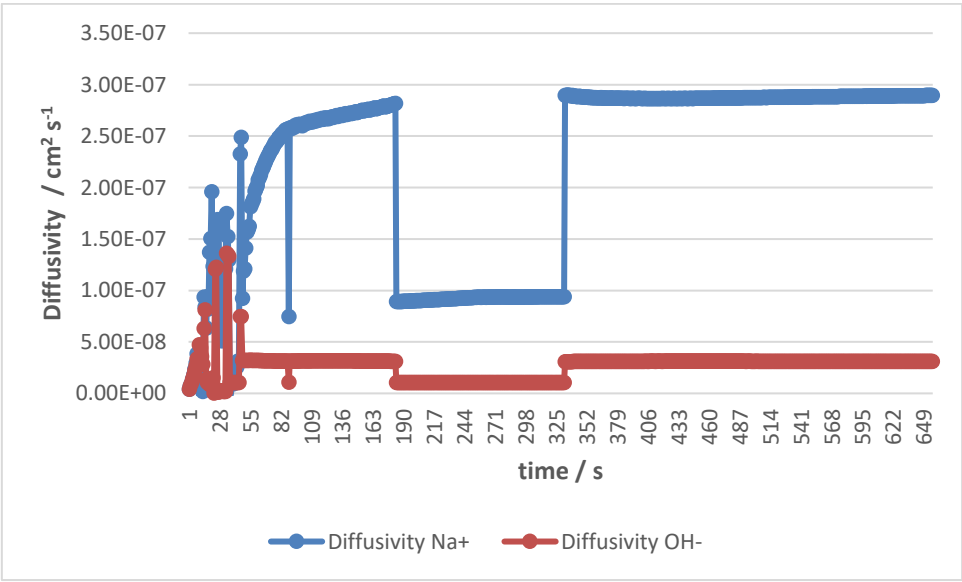

Figure 34 - Test 5, diffusivities values using a diffusivities finder in Python code.

Some problems happened after the 325th iteration, because it had already values stabilized at:

D_{Na+} [cm²/s] = 9.38E-08

D_{OH-} [cm²/s] = 1.05E-08

Test 6

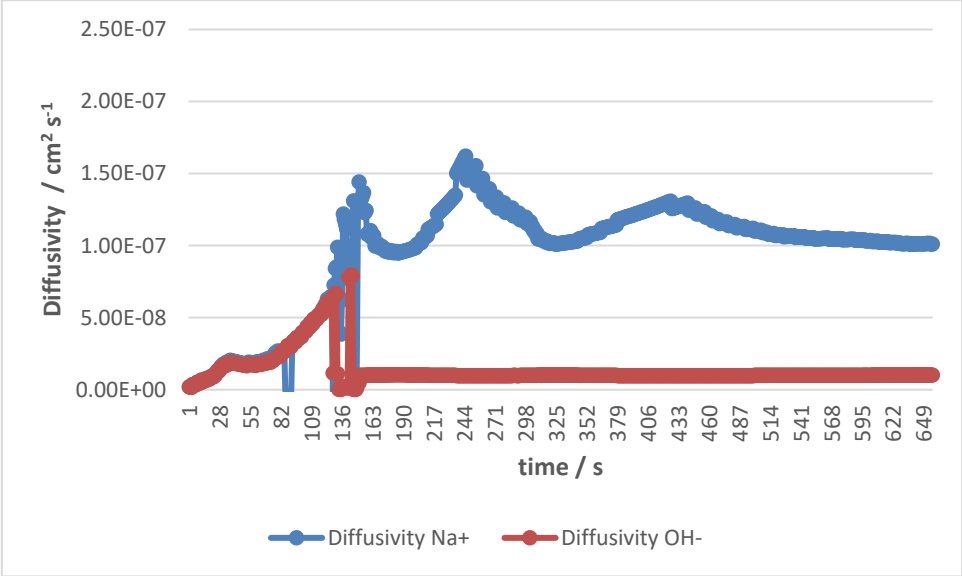

Figure 35 - Test 6, diffusivities values using a diffusivities finder in Python code.

From Figure 35, values are stabilized at:

D_{Na+} [cm^2/s] = 1.01E-07

D_{OH-} [cm^2/s] = 1.01E-08

Test 7

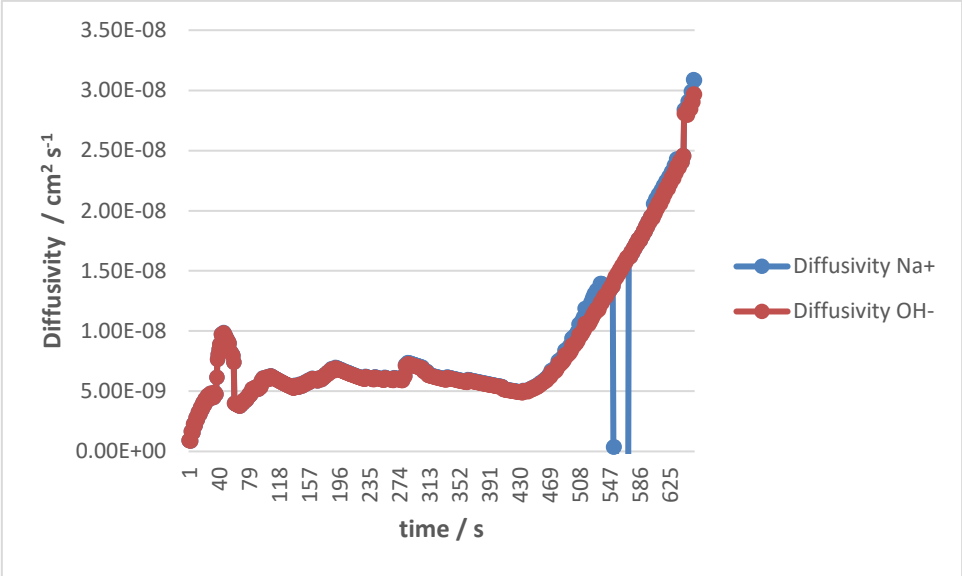

Figure 36 - Test 7, diffusivities values using a diffusivities finder in Python code.

From Figure 36, values are not stabilized.

Test 8

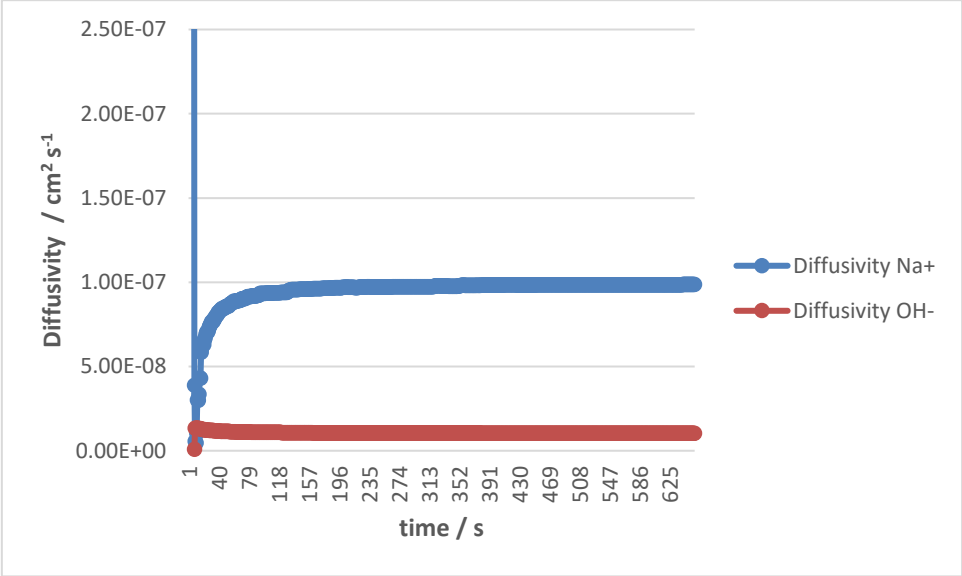

Figure 37 - Test 8, diffusivities values using a diffusivities finder in Python code.

From Figure 37, values are stabilized at:

D_{Na+} [cm^2/s] = 9.86E-08

D_{OH-} [cm^2/s] = 1.03E-08

Test 9

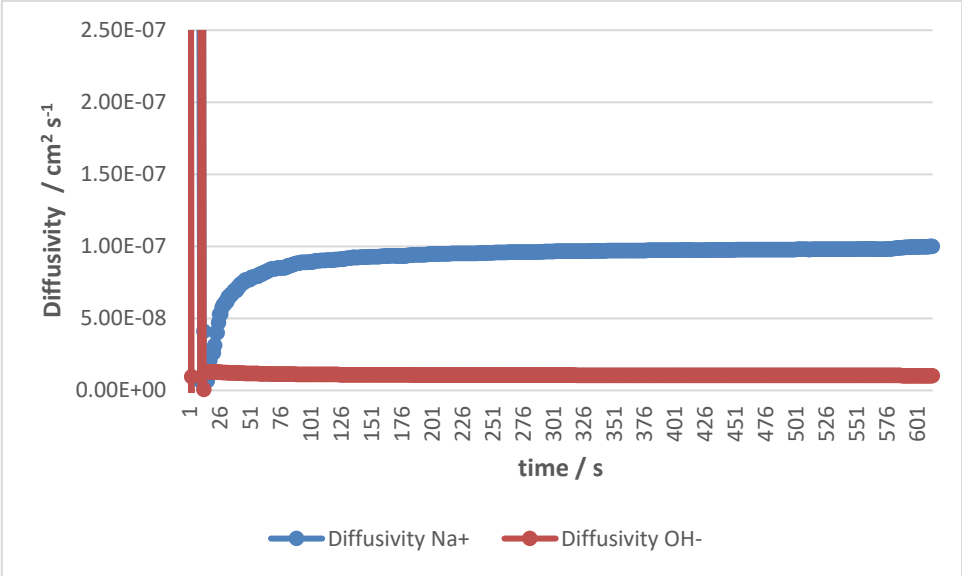

Figure 38 - Test 9, diffusivities values using a diffusivities finder in Python code.

From Figure 39, values are stabilized at:

D_{Na+} [cm^2/s] = 9.99E-08

D_{OH-} [cm^2/s] = 1.02E-08

Test 10

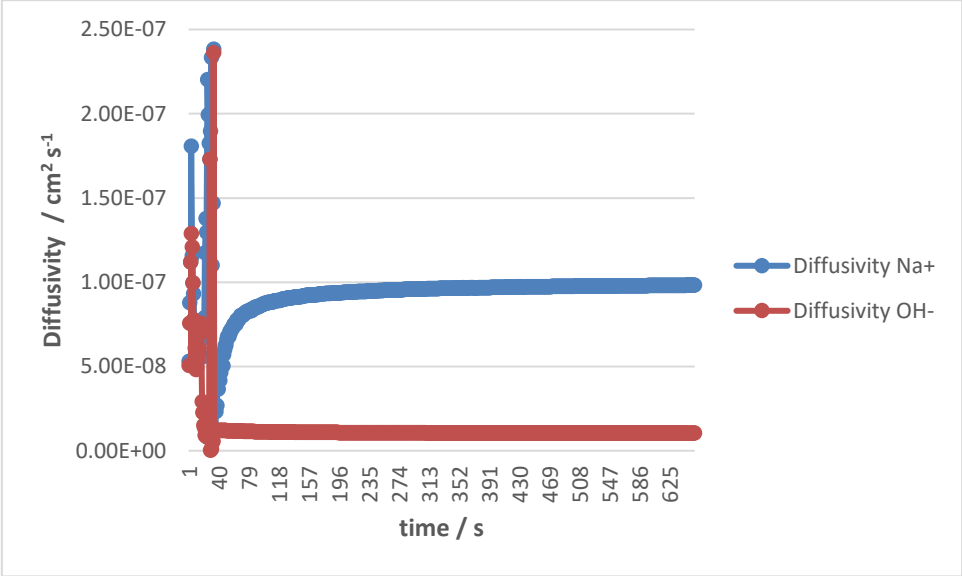

Figure 39 - Test 10, diffusivities values using a diffusivities finder in Python code.

From Figure 39, values are stabilized at:

D_{Na+} [cm^2/s] = 9.81E-08

D_{OH-} [cm^2/s] = 1.04E-08

Test 11

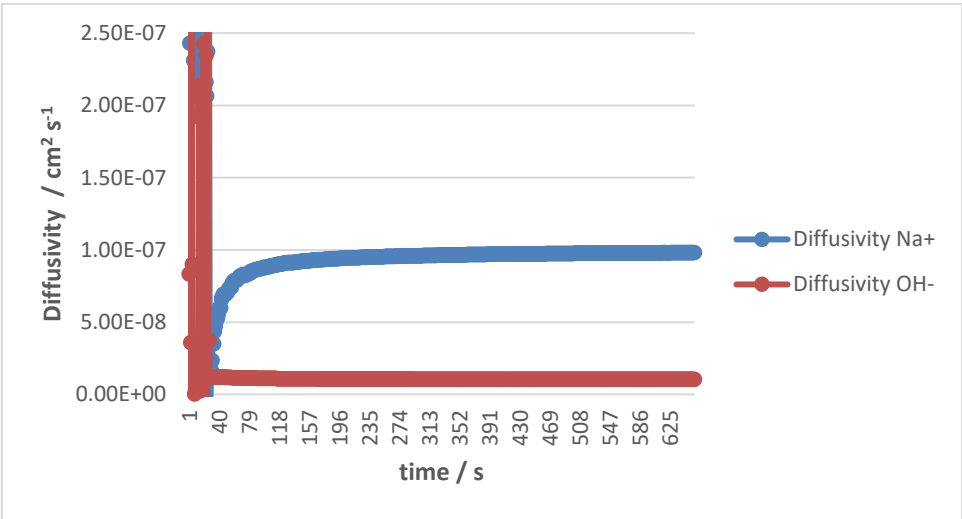

Figure 40 - Test 11, diffusivities values using a diffusivities finder in Python code.

From Figure 40, values are stabilized at:

D_{Na+} [cm^2/s] = 9.82E-08

D_{OH-} [cm^2/s] = 1.04E-08

Table 9 - Resume Diffusivities Table.

Test	D_{Na+} [cm^2/s]	D_{OH-} [cm^2/s]
1	1.00E-07	1.02E-08
2	1.00E-07	1.02E-08
3	1.00E-07	1.02E-08
4	9.95E-08	1.02E-08
5	NaN	NaN
6	1.01E-07	1.01E-08
7	NaN	NaN
8	9.86E-08	1.03E-08
9	9.99E-08	1.02E-08
10	9.81E-08	1.04E-08
11	9.82E-08	1.04E-08

From Table 9, some bullet points can be highlighted:

- the last two experiments (test 10 and 11) are the most trustable (because the last ones are made with nitrogen bubbling, and we have a confirmation of the tests from the overlayed pH measurements)
- in the most trustable experiments, an asymptote for each ion diffusivity can be spot, so after an initial time of stabilization, the diffusivity is roughly stabilized to a value
- also, the other tests give use similar stabilized values (except for tests 5 and 7, which could have some problems/contaminations in the measurement part)
- the diffusivity of Na^+ in Nafion N117 is very near to 9.82E-08 cm^2s^{-1}, and diffusivity of OH^- is very near to 1.04E-08 cm^2s^{-1} in each experiment (also in the first ones with not so many values measured)

More consistent results were expected, also using different non-linear methods to resolve the Nernst-Planck equations (easily implemented just activating them in the code created), but the outputs are influenced by the initial guess. Better initial values will give us better outputs values.

In the subsystem considered, it seems that OH^- diffusivity is one order-of-magnitude lower than the one

of Na^+, which is against most experimental evidence in systems with aqueous solutions. But the ion diffusivity inside the membrane is different from the ion diffusivity in the solutions: the difference between the two diffusivities inside the membrane were expected to be so different, because anions were supposed be hindered in CEMs(like Nafion N117).

Currently, in literature, only thresholds (and reference values) referring to some molecules are available, and this is the first attempt to define the single spitted ions diffusivity inside the specific membrane: not having diffusivity vales as a starting point, these values must be seen as the first starting point to improve in the next future.

Another Excel file was created to calculate the flux inside the membrane in a linear way (considering the nominal fixed charge of the membrane and computing the concentration of Na^+ and OH^- inside that), but also this excel file is influenced by the initial diffusivity guess used.

So, the results are not perfect, that is why the diffusivities found will be called “effective diffusion coefficients”: in any case the values are supported from real data taken from the experiments. The results are of course function of the temperature that has been recorded second by second in the experiments, and the idea is that this simple experiment will be replicated to get more trustable diffusivity values for the ions involved, to create an ion diffusivity function of temperature, and then pass to perform similar experiment also to the others ions involved (from the others subsystems). The information gathered from more experiments will be fundamental to having a diffusivity function for each ion and each membrane involved. Once the diffusivity inside the membrane function of temperature will be defined for each split Ions, at that point we could neglect the new definition of “effective” diffusion coefficient, because at that point that will be the proper diffusion coefficient (that matches both theoretical and experimental methods).

Chapter 4

Conclusions and future work

In the thesis, the concept that selective membrane blocking opposite charge ions was better elucidated, because each ion will pass inside. The whole molecule will pass through the membrane only when dissociated in ions, with the same velocity due to the membrane potential gradient (when an external electrical field is not applied in the region).

A theoretical model to understand the whole system of a DBPFC has been proposed, considering Nernst-Planck equations for each sub-system, with only one component per time, and having in mind the flux direction of the whole fuel cell.

Experimental tests were performed, to show the importance of the membrane potential, and to prove that negative ions will pass through a CEM membrane (in this case Nafion N117). These data have been used to feed a Python code, to make an estimation of the effective diffusion coefficients of NaOH in Nafion N117, and obtain a rough approximation of Na^+ to 9.82E-08 cm^2s^{-1}, and of OH^- to 1.04E-08 cm^2s^{-1}, at ambient temperature.

With better initial guessing values a better accuracy could be reached, but nobody has ever tested something like this, so the values found will be the first initial guess for the ones that will have more accurate values in the future. An outstanding accuracy cannot be reached for these results if the initial data are rough measurements in the lab. The critical parameter remains the diffusivity, and the key to resolve the system is to perform more similar experiments, to have a whole diffusivity function of temperature for each ion (and for each membrane, because of the diffusivity of the same ions could change between a CEM and an AEM).

So, this is the first step to define a general DBPFC model with diffusivity inside the membrane, applicable also to other liquid fuel cells. Thus, this must be seen as a starting point for a creation of a numerical model where liquid solutions are involved, and this work paved the basement to reach a deep knowledge of the membrane mechanisms inside the DBPFCs, pushing the borders of their actual State-of-the-Art.

For future development, the way to reach the creation of a CFD model was shown (once all the diffusivities involved have been found). With the creation of new information also a machine learning algorithm could be implemented, to get more insight from the mole of data created. In addition, numerical optimization of the cell will lead also to the creation of new high-performance DBPFC, thanks to 3D printing.

References

[1] *Chapter 10 - Direct borohydride fuel cell (DBFCs)*; B. Sljukic and D.M.F. Santos, Direct Liquid Fuel Cells: Fundamentals, Advances and Future; Edited by Ramiz Gultekin Akay and Ayse Bayrakceken Yurtcan; Elsevier, Academic Press; ISBN: 978-0-12-818624-4; (2021).

[2] *Simple design of PVA-based blend doped with $SO_4(PO_4)$-functionalised TiO_2 as an effective membrane for direct borohydride fuel cells*. M.H. Gouda, W. Gouveia, N.A. Elessawy, B. Sljukic, A.B.A.A. Nassr, D.M.F. Santos, Int J Hydrogen Energy 2020;45:15226–38 (2020). https://doi.org/10.1016/j.ijhydene.2020.04.013

[3] *Anion- or cation-exchange membranes for $NaBH_4/H_2O_2$ fuel cells?*; B. Sljukic, A.L. Morais, D.M.F. Santos, C.A.C Sequeira., Membranes 2012;2:478–92, Vol. 2, 3, 478-492 (2012). http://dx.doi.org/10.3390/membranes2030478

[4] *Efficient pH-gradient-enabled microscale bipolar interfaces in direct borohydride fuel cells* Z. Wang, J. Parrondo, C. He, S. Sankarasubramanian, V. Ramani, Nat Energy 2019;4:281–9. (2019)

[5] *Effect of Membrane Separators on the Performance of Direct Borohydride Fuel Cells*, D.M.F. Santos and C.A.C. Sequeira, Journal of The Electrochemical Society, 159 (2) B126-B132 (2012)

[6] *Ionic Liquid-Derived Carbon-Supported Metal Electrocatalysts as Anodes in Direct Borohydride-Peroxide Fuel Cells*, J. Milikic, R.C.P. Oliveira, A. Tapia, D.M.F. Santos, N. Zdolšek, T. Trtic Petrovic, M. Vraneš, B. Šljukic, Catalysts 11, 632. (2021) https:// doi.org/10.3390/catal11050632

[7] *Poly(vinyl alcohol)-based crosslinked ternary polymer blend doped with sulfonated graphene oxide as a sustainable composite membrane for direct borohydride fuel cells,* M.H. Gouda, W. Gouveia, M.L. Afonso, B. Šljukić, N.A. El Essawy, A.B.A.A. Nassr, and D.M.F. Santos, Journal of Power Sources, Vol. 432, 92-101 (2019). https://doi.org/10.1016/j.jpowsour.2019.05.078

[8] *OpenFuelCell: List of Publications*, https://openfuelcell.sourceforge.io/publications (available online, visited on 5/8/ 2021)

[9] *Computational study of heat and mass transfer issues in solid oxide fuel cells*, D.H. Jeon, S.B. Beale , H-W Choi , J.G. Pharoah and H. Roth, The 21st International Symposium on Transport Phenomena November 2-5, (2010), https://www.researchgate.net/profile/Jg-Pharoah/publication/48446431_Computational_study_of_heat_and_mass_transfer_issues_in_solid_oxide_fuel_cells/links/00b7d525f798d9fc43000000/Computational-study-of-

heat-and-mass-transfer-issues-in-solid-oxide-fuel-cells.pdf

[10] *Effect of Porous Microstructural Properties on the Results of a Cell-Level Model in Solid Oxide Fuel Cells*, H-W Choi, A. Berson, J. Pharoah and S. Beale, ECS - The Electrochemical Society ECS Transactions, Volume 35, Number 1, (2011) https://iopscience.iop.org/article/10.1149/1.3570091/pdf?casa_token=yOZ8Z2gCvU8AAAAA:Fa2817BbDI4xEFaKlGkTYZ9Jf4QiACU5ns3MyICvnzRFyD-4_izC66xGRTBeeiu6y67w5vQ5961ldJcxD7pcAw8

[11] *Numerical and Experimental Analysis of a Solid Oxide Fuel Cell Stack*, S. Beale, A. D. Le, H. Roth, J. Pharoah, H-W Choi, L.G.J. De Haart and D. Froning, ECS - The Electrochemical Society ECS Transactions, Volume 35, Number 1, (2011) https://iopscience.iop.org/article/10.1149/1.3570074/pdf?casa_token=ux2CaMF_TgAAAAAA:XypFdxw0KdZjDnmKlehomX1hsRwZfeqWwhZwLf7c7iX_gRp7n_JjWKjDd4TzixWv5OViXYtr1PiZGkGymsvwOK4

[12] *Impact of Manifolding on Performance of a Solid Oxide Fuel Cell Stack*, R. Nishida, S. Beale, and Jon G. Pharoah, ECS - The Electrochemical Society ECS Transactions, Volume 57, Number 1, (2013) https://iopscience.iop.org/article/10.1149/05701.2495ecst/pdf

[13] *The Development of a Coupled Physics and Kinetics Model to Computationally Predict the Powder to Power Performance of Solid Oxide Fuel Cell Anode Microstructures*, D. Albert, W. Gawel, Queen's University Kingston, Ontario, Canada September (2013), https://qspace.library.queensu.ca/bitstream/handle/1974/8399/Gawel_Duncan_A_W_201309_MASc.pdf?sequence=1&isAllowed=y

[14] *Comparison of Solid Oxide Fuel Cell Stack Performance Using Detailed and Simplified Models*, R. T. Nishida, S. B. Beale, J. G. Pharoah, FuelCell2013-18137, V001T02A004; 10 pages, December 22, (2013), https://doi.org/10.1115/FuelCell2013-18137

[15] *The Importance of Diffusion Mechanisms in High Temperature Polymer Electrolyte Fuel Cells*, Q. Cao, S. B. Beale, U. Reimer, D. Froning and W. Lehnert, ECS - The Electrochemical Society ECS Transactions, Volume 69, Number 17 (2015), https://iopscience.iop.org/article/10.1149/06917.1089ecst/pdf

[16] *Development of a SOFC Performance Model to Analyze the Powder to Power Performance of Electrode Microstructures*, A.W. Duncan, J. Gawel, G. Pharoah and S. B. Beale, ECS - The Electrochemical Society ECS Transactions, Volume 68, Number 1 (2015) https://iopscience.iop.org/article/10.1149/06801.1979ecst/pdf?casa_token=p6FKMOc-dBEAAAAA:tb34pCdRzP0R4BO0lOl9yRhjnVzKWBGLcROjDu-TAdpExgKCgWeuK_Vv2z2HuQrCEWR3sKajo-N37pZzWSYlR1E

[17] *Computational Fluid Dynamics Modelling of Solid Oxide Fuel Cell Stacks*, R. T. Nishida, December 2 (2013), https://qspace.library.queensu.ca/handle/1974/8379

[18] *Three-dimensional computational fluid dynamics modelling and experimental validation of*

the Jülich Mark-F solid oxide fuel cell stack, R.T. Nishida, S.B. Beale, J.G. Pharoah, L.G.J. de Haart and L. Blum, Journal of Power Sources Volume 373, Pages 203-210, January 1 (2018), https://doi.org/10.1016/j.jpowsour.2017.10.030

[19] *Numerical Modeling of Anode-Supported Solid Oxide Fuel Cell Using Openfoam*, D. H. Jeon, S-B Lee, J-E Hong and R-H Song, ECS - The Electrochemical Society ECS Meeting Abstracts, Volume MA2019-01, F04-Multiscale Modeling, Simulation and Design 3: Enhancing Understanding, and Extracting Knowledge from Data, (2019), https://iopscience.iop.org/article/10.1149/MA2019-01/22/1144/meta

[20] *Open-source computational model of a solid oxide fuel cell*, S. B. Beale, H-W Choi, J. G. Pharoah, H. K. Roth, H. Jasak and D. H. Jeon, October 30 (2015), https://www.sciencedirect.com/science/article/abs/pii/S0010465515003872?casa_token=AsKAHZ4dvAsAAAAA:EvpF8lRmU5BHS_7WZI0iPCQzS59A6W-fsZa91HKH2O6qCAx-H3w6rp3yoxKbTWvXxecFwSiYJg

[21] *OpenFuelCell: Project*, (available online, visited on 5/8/2021) http://openfuelcell.sourceforge.net/

[22] *Documentation: sofcFoam.C*, (available online, visited on 5/8/2021) https://openfuelcell.sourceforge.io/doc/sofcfoamc

[23] *An openFuelCell tutorial*, H. Grimler, D. Segersson and M. Arabnejad, December 12 (2017), http://www.tfd.chalmers.se/~hani/kurser/OS_CFD_2017/HenrikGrimler/report_Grimler.pdf

[24] *CFD modeling and simulation of PEM fuel cell using OpenFOAM*, J-P Kone, X. Zhang, Y. Yan, G. Hu and G. Ahmadi, Energy Procedia Volume 145, , Pages 64-69, July (2018), https://www.sciencedirect.com/science/article/pii/S1876610218300122

[25] *An Open-Source Toolbox for PEM Fuel Cell Simulation*, J-P Kone, X. Zhang, Y. Yan and S. Adegbite, Published: May 10 (2018), https://www.mdpi.com/2079-3197/6/2/38

[26] *An Open-Source Toolbox for Multiphase Flow Simulation in a PEM Fuel Cell*, J-P Kone, X. Zhang, Y. Yan and S. Adegbite, Computer and Information Science; Vol. 11, No. 3; 2018 ISSN 1913-8989 E-ISSN 1913-8997 Published by Canadian Center of Science and Education, Online Published: May 21 (2018), https://pdfs.semanticscholar.org/9ced/776a6b3d5f933d0dcfe67b783c2d68989b68.pdf

[27] *Optimum supply and utilization of pure oxygen along with nitrogen on the cathode side for thermal stability of a proton exchange membrane fuel cell*, R. Gadhewal, S. K. Thamida, V. and V. Ananthula, Published online: Oct 5 (2019), https://www.tandfonline.com/doi/abs/10.1080/02286203.2019.1674766

[28] *CFD modeling and simulation of PEM fuel cell using OpenFOAM*, (available online, visited on 5/8/2021), https://www.researchgate.net/publication/326800168_CFD_modeling_and_simulation_of

_PEM_fuel_cell_using_OpenFOAM

[29] *Open Source PEM Cell Simulation Tool: opem1.3*, (available online, visited on 5/8/2021), https://pypi.org/project/opem/

[30] *Improve Energy Efficiencies with the Fuel Cell & Electrolyzer Module*, (available online, visited on 5/8/2021), https://www.comsol.com/fuel-cell-and-electrolyzer-module

[31] *CFD simulations about cooling a Proton Exchange Membrane fuel cell PEM and its stack in Ansys Fluent*, Ahmed Mansour, (available online, visited on 5/8/2021), https://www.youtube.com/watch?v=HX9a5uijvF0

[32] *Fuel Cell Stack*, (available online, visited on 5/8/2021), https://www.mathworks.com/help/physmod/sps/powersys/ref/fuelcellstack.html

[33] *Ansys Student Software: Ansys Student*, (available online, visited on 5/8/2021), https://www.ansys.com/academic/students/ansys-student

[33] *Anion Partitioning in and Diffusion through a Nafion Membrane*, K-L Huang, T. M. Holsen, and J. R. Selman, *Eng. Chem. Res.* 42, 15, 3620–3625, (2003), https://doi.org/10.1021/ie030109q

[34] *Ion mobility in Nafion-117 membranes*, I. A. Stenina, P. Sistat, A.I. Rebrov, G. Pourcelly and Y. Andrey, Desalination 170(1):49-57, October (2004) https://www.researchgate.net/publication/229305822_Ion_mobility_in_Nafion-117_membranes

[35] *Ionic Transport Processes In Electrochemistry and Membrane Science*, K. Kontturi, L. Murtomaki and J. A. Manzanares, Oxford University Press, (2008)

Annex A

Membrane potential and concentration inside the membrane

A.1.1 Concentration profile inside the membrane

To understand the profile of the membrane potential inside the membrane (as a function of the membrane thickness, in the x-axis direction), a solved example is shown (Figure A.1):

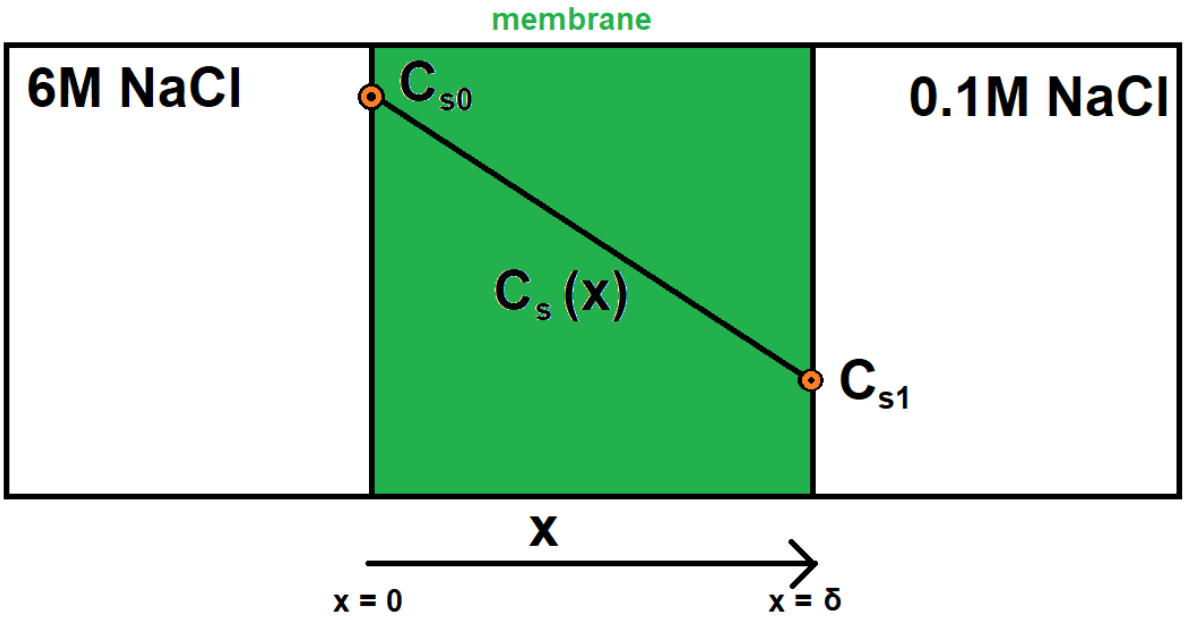

Figure A.1 - Membrane example: 6 M NaCl and 0.1 M NaCl, divided by a membrane.

The same salt is present in two different compartments, separated by a membrane of known thickness (δ), but with two different concentrations of the salt.

The understanding of the whole process could be deepened by reading the relative chapters of *Ionic Transport Processes In Electrochemistry and Membrane Science* [35].

What happens inside the membrane can be explained by the Nernst-Planck equations for the ions involved (where the positive subscript refers to the positive ion Na^+, and the negative subscript refers to the negative ion Cl^-), not considering the convection term of the equations (Eq. 101 and 102):

$$N^+ = -D^+ \frac{dC_s(x)}{dx} - C_s(x) D^+ \frac{F}{R*T} \frac{d\Psi(x)}{dx} \quad (101)$$

$$N^- = -D^- \frac{dC_s(x)}{dx} + C_s(x) D^- \frac{F}{R*T} \frac{d\Psi(x)}{dx} \quad (102)$$

Due to the electroneutrality of the solutions, the flux can be expressed in Eq. 103:

$$N^+ = N^- = N \quad (103)$$

So, the Nernst-Planck equations become (Eq. 104 and 105):

$$N = -D^+ \frac{dC_s(x)}{dx} - C_s(x) D^+ \frac{F}{R*T} \frac{d\Psi(x)}{dx} \quad (104)$$

$$N = -D^{-}\frac{dC_s(x)}{dx} + C_s(x)D^{-}\frac{F}{R*T}\frac{d\Psi(x)}{dx} \quad (105)$$

There is the first equation for D^+ (Eq. 106), and the second equation per D^- (Eq. 107)

$$\frac{N}{D^+} = -\frac{dC_s(x)}{dx} - C_s(x)\frac{F}{R*T}\frac{d\Psi(x)}{dx} \quad (106)$$

$$\frac{N}{D^-} = -\frac{dC_s(x)}{dx} + C_s(x)\frac{F}{R*T}\frac{d\Psi(x)}{dx} \quad (107)$$

The two equations have as unknowns Ψ(x) and C_s(x).

These two last equations can be *summed* (Eqs. 108-110), to obtain only one equation with the unknown concentration C_s(x):

$$\frac{N}{D^+} + \frac{N}{D^-} = -2\frac{dC_s(x)}{dx} \quad (108)$$

$$\frac{N*(D^-+D^+)}{D^+*D^-} = -2\frac{dC_s(x)}{dx} \quad (109)$$

$$\frac{dC_s(x)}{dx} = -\frac{N*(D^-+D^+)}{2*D^+*D^-} \quad (110)$$

Considering the diffusivities and the flux constant inside the membrane, the second term can be simplified in another constant A (Eq. 111):

$$A = \frac{N*(D^-+D^+)}{2*D^+*D^-} \quad (111)$$

To obtain Eq. 112:

$$\frac{dC_s(x)}{dx} = -A \quad (113)$$

With a general integration it becomes (Eq. 113):

$$C_s(x) = -A*x + B \quad (113)$$

Using the boundary conditions (Eq. 114 and 115):

$$C_s(0) = C_{s0} \quad (114)$$

$$C_s(\delta) = C_{s1} \quad (115)$$

The integration constant B can be known as.

At x=0, $C_s(0) = C_{s0}$ so $B = C_{s0}$

At x= δ, $C_s(\delta) = C_{s1}$ so $C_{s1} = -A*\delta + C_{s0}$

To have the profile of the concentration inside the membrane (Eq. 116):

$$C_s(x) = C_{s0} - A*\mathrm{x} \quad (116)$$

A.1.2 Membrane potential profile inside the membrane

The first equation is divided per D^+, and the second equation per D^- (Eq. 117 and 118)

$$\frac{N}{D^+} = -\frac{dC_s(x)}{dx} - C_s(x)\frac{F}{R*T}\frac{d\Psi(x)}{dx} \tag{117}$$

$$\frac{N}{D^-} = -\frac{dC_s(x)}{dx} + C_s(x)\frac{F}{R*T}\frac{d\Psi(x)}{dx} \tag{118}$$

The two equations have as unknowns $\Psi(x)$ and $C_s(x)$.

The first and the second equation can be *subtracted* (Eq. 119), to obtain only one equation with the unknown of the membrane potential $\Psi(x)$:

$$\frac{N}{D^+} - \frac{N}{D^-} = -2C_s(x)\frac{F}{R*T}\frac{d\Psi(x)}{dx} \tag{119}$$

After some mathematical passages to obtain the membrane potential explicitly on the left part (Eq. 120 and 121):

$$\frac{N*(D^- - D^+)}{D^+*D^-} = -2C_s(x)\frac{F}{R*T}\frac{d\Psi(x)}{dx} \tag{120}$$

$$\frac{d\Psi(x)}{dx} = \frac{R*T}{2FC_s(x)} * \frac{N*(D^+ - D^-)}{D^+*D^-} \tag{121}$$

A new constant β (V mol m^{-4}) can be expressed as (Eq. 122):

$$\beta = \frac{R*T}{2F} * \frac{N*(D^+ - D^-)}{D^+*D^-} \tag{122}$$

to obtain (Eq. 123):

$$\frac{d\Psi(x)}{dx} = \frac{\beta}{C_s(x)} \tag{123}$$

The concentration profile already found is (Eq. 124):

$$C_s(x) = C_{s0} - A * \mathrm{x} \tag{124}$$

With the parameter (Eq. 125):

$$A = \frac{N*(D^- + D^+)}{2*D^+*D^-} \tag{125}$$

To obtain the expression of $\Psi(x)$, the boundary conditions are used (Eqs. 126-131):

$$C_s(0) = C_{s0} \tag{126}$$

$$C_s(\delta) = C_{s1} \tag{127}$$

$$\Delta C_s = C_{s1} - C_{s0} \tag{128}$$

$$\Psi(0) = \Psi_0 \tag{129}$$

$$\Psi(\delta) = \Psi_1 \tag{130}$$

$$\Delta\Psi = \Psi_1 - \Psi_0 \tag{131}$$

Some mathematical passages are made (Eqs. 132-134):

$$\frac{d\Psi(x)}{dx} = \frac{\beta}{C_s(x)} \tag{132}$$

$$\frac{d\Psi(x)}{dx} = \frac{\beta}{C_{s0} - A*\mathrm{x}} \tag{133}$$

$$\Psi(x) = \int \frac{\beta}{C_{s0} - A*\mathrm{x}} dx \tag{134}$$

And having a substitution (Eqs. 135-137):

$$u = C_{s0} - A * \mathrm{x} \tag{135}$$

$$\frac{du}{dx} = -A \tag{136}$$

$$dx = -\frac{1}{A}\, du \tag{137}$$

To obtain Eq. 138 and 139:

$$\Psi(x) = \int \frac{\beta}{u} * \left(-\frac{1}{A}\right) du \tag{138}$$

$$\Psi(x) = -\frac{\beta}{A} \int \frac{1}{u}\, du \tag{130}$$

Knowing that: $\int \frac{1}{u} du = \ln(u)$, the profile is found (Eq. 140):

$$\Psi(x) = -\frac{\beta}{A} * \ln(C_{s0} - A * \mathrm{x}) + B \tag{140}$$

To have the constant of integration B, the boundary condition is used:

At x=0, $\Psi(0) = \Psi_0$ so $B = \Psi_0 + \frac{\beta}{A} * \ln(C_{s0})$

So, the profile becomes (Eq. 141):

$$\Psi(x) = -\frac{\beta}{A} * \ln(C_{s0} - A * \mathrm{x}) + \Psi_0 + \frac{\beta}{A} * \ln(C_{s0}) \tag{141}$$

That can be reshaped in (Eq. 142):

$$\Psi(x) = \Psi_0 + \frac{\beta}{A} * [\ln(C_{s0}) - \ln(C_{s0} - A * \mathrm{x})] \tag{142}$$

Knowing that $\ln(a) - \ln(b) = \ln\left(\frac{a}{b}\right)$

So, the membrane potential inside the membrane (Eq. 143) is:

$$\Psi(x) = \Psi_0 + \frac{\beta}{A} * \left[\ln\left(\frac{C_{s0}}{C_{s0} - A*\mathrm{x}}\right)\right] \tag{143}$$

A.1.3 Alternative Membrane Potential profile inside the membrane

A different profile of concentration inside the membrane can be used, a more general profile like (Eq. 144):

$$C_s(x) = C_{s0} - \frac{x}{\delta}(C_{s0} - C_{s1}) \tag{144}$$

To substitute in the differential equation (Eq. 145):

$$\frac{d\Psi(x)}{dx} = \frac{\beta}{C_s(x)} \tag{145}$$

To obtain the expression of Ψ(x), using the boundary conditions (Eqs. 146-151):

$$C_s(0) = C_{s0} \tag{146}$$

$$C_s(\delta) = C_{s1} \tag{147}$$

$$\Delta C_s = C_{s1} - C_{s0} \tag{148}$$

$$\Psi(0) = \Psi_0 \tag{149}$$

$$\Psi(\delta) = \Psi_1 \tag{150}$$

$$\Delta\Psi = \Psi_1 - \Psi_0 \tag{151}$$

After some mathematical passages (Eqs. 152-154):

$$\frac{d\Psi(x)}{dx} = \frac{\beta}{C_s(x)} \tag{152}$$

$$\frac{d\Psi(x)}{dx} = \frac{\beta}{C_{s0} - \frac{x}{\delta}(C_{s0} - C_{s1})} \tag{153}$$

$$\Psi(x) = \int \frac{\beta}{C_{s0} - \frac{x}{\delta}(C_{s0} - C_{s1})} dx \tag{154}$$

It is possible a substitution (Eqs. 155-157):

$$u = C_{s0} - \frac{x}{\delta}(C_{s0} - C_{s1}) \tag{155}$$

$$\frac{du}{dx} = -\frac{(C_{s0} - C_{s1})}{\delta} \tag{156}$$

$$dx = -\frac{\delta}{(C_{s0} - C_{s1})}\, du \tag{157}$$

To obtain Eq. 158 and 159:

$$\Psi(x) = \int \frac{\beta}{u} * \left(-\frac{\delta}{(C_{s0} - C_{s1})}\right) du \tag{158}$$

$$\Psi(x) = -\frac{\beta*\delta}{(C_{s0}-C_{s1})}\int \frac{1}{u}\, du \tag{159}$$

Knowing that: $\int \frac{1}{u} du = \ln(u)$, the profile becomes (Eq. 160):

$$\Psi(x) = -\frac{\beta*\delta}{(C_{s0}-C_{s1})} * \ln\left(C_{s0} - \frac{x}{\delta}(C_{s0}-C_{s1})\right) + B \tag{160}$$

To have the constant of integration B, the boundary condition used is:

At x=0, $\Psi(0) = \Psi_0$ so $B = \Psi_0 + \frac{\beta*\delta}{(C_{s0}-C_{s1})} * \ln(C_{s0})$

So, the profile is (Eq. 161):

$$\Psi(x) = -\frac{\beta*\delta}{(C_{s0}-C_{s1})} * \ln\left(C_{s0} - \frac{x}{\delta}(C_{s0}-C_{s1})\right) + \Psi_0 + \frac{\beta*\delta}{(C_{s0}-C_{s1})} * \ln(C_{s0}) \tag{161}$$

That can be reshaped in (Eq. 162):

$$\Psi(x) = \Psi_0 + \frac{\beta*\delta}{(C_{s0}-C_{s1})} * \left[\ln(C_{s0}) - \ln\left(C_{s0} - \frac{x}{\delta}(C_{s0}-C_{s1})\right)\right] \tag{162}$$

Knowing that $\ln(a) - \ln(b) = \ln\left(\frac{a}{b}\right)$

The membrane potential inside the membrane is (Eq. 163):

$$\Psi(x) = \Psi_0 + \frac{\beta*\delta}{(C_{s0}-C_{s1})} * \left[\ln\left(\frac{C_{s0}}{C_{s0}-\frac{x}{\delta}(C_{s0}-C_{s1})}\right)\right] \tag{163}$$

So, the final form of the membrane potential (Eq. 164) and the concentration (Eq. 165), are:

$$\Psi(x) = \Psi_0 + \frac{\beta*\delta}{(C_{s0}-C_{s1})} * \left[\ln\left(\frac{C_{s0}}{C_{s0}\left(1-\frac{x}{\delta}\right)+\frac{x}{\delta}*C_{s1}}\right)\right] \tag{164}$$

$$C_s(x) = C_{s0} - \frac{x}{\delta}(C_{s0}-C_{s1}) \tag{165}$$

These are different from the profiles found in the last chapter:

$$\Psi(x) = \Psi_0 + \frac{\beta}{A} * \left[\ln\left(\frac{C_{s0}}{C_{s0}-A*\mathrm{x}}\right)\right] \tag{143}$$

$$C_s(x) = C_{s0} - A*\mathrm{x} \tag{116}$$

Annex B

Python Code Explanation

B.2.1 Python code

The following is the python code used to find diffusivities inside the Nafion N117 membrane with the data taken from the experiments in the lab.

```
#concentration profile
#Cs (x)=Cs0  -A*x

#libraries used
import numpy as np
from scipy.optimize import fsolve
from scipy import optimize
from scipy.optimize import minimize, rosen, rosen_der, rosen_hess
import pandas as pd
import math
import csv

#constant defined
Cs0 = 0.004  # initial concentration NaOH= 0,004 [mol/cm3]= 4 M
Volume = 75  # volume of solution 75 mL =75 cm3
Area_mem = 6.5 * 4.5  # active membrane area = 29,25 cm2
thick = 0.0208  # Nafion N117 hydrated thickness [cm]
R = 8.31446261815324  # Gas Constant R [J/(mol*K)]
F = 96485.3365  # Faraday Constant F [C/mol]

#parameters from excel file
bids = pd.read_excel("test12.xlsx") #open excel file with only values of T [C], N [mol/(cm2*s)], Cs1 [mol/cm3] and deltaC [-]
c=bids.to_numpy() #to select later only the specific column in the excel file
```

```
#function defined: two Nernst-Planck equation with the unknow (D1,D2)=(x[0],x[1)]
def func(x):
    beta = R * T * N * ((x[0] - x[1]) / (x[0] * x[1])) / (2 * F) #beta=[V*mol/cm4]
    A= N*((x[0] + x[1]) / (2*x[0] * x[1])) # A=[mol/cm4]
    Z=Cs0-(A*thick) #z=[mol/cm3]
    Psi = beta*thick/Cs1 #Psi=[V]

    #Psi = (beta/A)*(math.log(Cs0 / (Cs0-(A*thick))))
    #0= N -x[0] * (-deltaC) / thick - Cs1 * x[0] * F * Psi / (R * T * thick)
    #0= N -x[1] * (-deltaC) / thick + Cs1 * x[1] * F * Psi / (R * T * thick)

    return np.array([-N -x[0] * (-deltaC) / thick - Cs1 * x[0] * F * Psi / (R * T * thick) , -N -x[1] * (-deltaC) / thick + Cs1 * x[1] * F * Psi / (R * T * thick)] , dtype='float64' )

    #return np.array([-N -x[0] * (-deltaC) / thick - Cs1 * x[0] * F * (((R * T * N * ((x[0] - x[1]) / (x[0] * x[1])) / (2 * F))/(N*((x[0] + x[1]) / (2*x[0] * x[1])))*(math.log(Cs0 / (Cs0-(N*((x[0] + x[1]) / (2*x[0] * x[1])))*thick)))) / (R * T * thick) ,          -N -x[1] * (-deltaC) / thick + Cs1 * x[1] * F * (((R * T * N * ((x[0] - x[1]) / (x[0] * x[1])) / (2 * F))/(N*((x[0] + x[1]) / (2*x[0] * x[1])))*(math.log(Cs0 / (Cs0-(N*((x[0] + x[1]) / (2*x[0] * x[1])))*thick)))) / (R * T * thick)], dtype='float64' )
    #in the function "func(x)" we put both Nernst-Planck equations, separated by a comma
    #dtype('float64') --> # 64-bit floating-point number


#beta = R * T * N * ((D1 - D2) / (D1 * D2)) / (2 * F) #check that D1>D2, otherwise there is a division by zero
#A= N*((D1 + D2) / (2*D1 * D2))
#Psi = (beta/A)*(math.log(Cs0 / (Cs0-A*thick)))

#deltaC = Cs0 - Cs1

#Psi = ((R * T * N * ((D1 - D2) / (D1 * D2)) / (2 * F))/(N*((D1 + D2) / (2*D1 * D2))))*(math.log(Cs0 / (Cs0-(N*((D1 + D2) / (2*D1 * D2)))*thick)))
```

#Linearization of Nernst-Planck equations

#N1 = -D1 * (-deltaC) / thick - Cs1 * D1 * F * Psi / (R * T * thick)

#N2 = -D2 * (-deltaC) / thick + Cs1 * D2 * F * Psi / (R * T * thick)

(-deltaC) because the second term of the implicit equations must be positive, so the diffusion of Na^+ is slowed in the first equation and the diffusion of OH^- is accelerated in the second equation

the deltaC is calculated to be a positive term, but from a mathematical point of view Cs1-Cs0 give a negative value because we have a lower concentration in the second compartment

#substitution of Psi

#N1 = -D1 * (-deltaC) / thick - Cs1 * D1 * F * (((R * T * N * ((D1 - D2) / (D1 * D2)) / (2 * F))/(N*((D1 + D2) / (2*D1 * D2))))*(math.log(Cs0 / (Cs0-(N*((D1 + D2) / (2*D1 * D2)))*thick)))) / (R * T * thick)

#N2 = -D2 * (-deltaC) / thick + Cs1 * D2 * F * (((R * T * N * ((D1 - D2) / (D1 * D2)) / (2 * F))/(N*((D1 + D2) / (2*D1 * D2))))*(math.log(Cs0 / (Cs0-(N*((D1 + D2) / (2*D1 * D2)))*thick)))) / (R * T * thick)

#f=(f1,f2)

#f1=0= -N1 -D1 * (-deltaC) / thick - Cs1 * D1 * F * (((R * T * N * ((D1 - D2) / (D1 * D2)) / (2 * F))/(N*((D1 + D2) / (2*D1 * D2))))*(math.log(Cs0 / (Cs0-(N*((D1 + D2) / (2*D1 * D2)))*thick)))) / (R * T * thick)

#f2=0= -N2 -D2 * (-deltaC) / thick + Cs1 * D2 * F * (((R * T * N * ((D1 - D2) / (D1 * D2)) / (2 * F))/(N*((D1 + D2) / (2*D1 * D2))))*(math.log(Cs0 / (Cs0-(N*((D1 + D2) / (2*D1 * D2)))*thick)))) / (R * T * thick)

#electroneutrality in solutions

#N=N1=N2

#final implicit function equations:

#f=(f1,f2)

#f1=0= -N -D1 * (-deltaC) / thick - Cs1 * D1 * F * (((R * T * N * ((D1 - D2) / (D1 * D2)) / (2 * F))/(N*((D1 + D2) / (2*D1 * D2))))*(math.log(Cs0 / (Cs0-(N*((D1 + D2) / (2*D1 * D2)))*thick)))) / (R * T * thick)

#f2=0= -N -D2 * (-deltaC) / thick + Cs1 * D2 * F * (((R * T * N * ((D1 - D2) / (D1 * D2)) / (2 * F))/(N*((D1 + D2) / (2*D1 * D2))))*(math.log(Cs0 / (Cs0-(N*((D1 + D2) / (2*D1 * D2)))*thick)))) / (R * T * thick)

#with D1=x[0] --> Diffusivity of Na+ in Nafion membrane

```
# and D2=x[1] --> Diffusivity of OH- in Nafion membrane


# derivative of the objective function
def derivative(x):
    beta = R * T * N * ((x[0] - x[1]) / (x[0] * x[1])) / (2 * F)
    #A= N*((x[0] + x[1]) / (2*x[0] * x[1]))
    Psi = beta*thick/Cs1
    return [N - (deltaC) / thick - Cs1 * F * Psi / (R * T * thick) , N - (deltaC) / thick + Cs1 * F * Psi / (R * T * thick)]


#store variables
f = open('res11.csv', 'a',newline='') #newlines='' to avoid empty lines between results
# g = open('res2.csv', 'a')
#q = open('res3.csv', 'a',newline='')
# w = open('res4.csv', 'a')
writer1 = csv.writer(f) #save the results in the excel file
# writer2 = csv.writer(g)
#writer3 = csv.writer(q)
# writer4 = csv.writer(w)


#optimization
for i in range (1,900):     # To obtain the result of whole range, just put: """(0,len(c))"""
                        #the first 10 (11 if we start counting from 1 and not 0) are cut, because they show a negative flow than lead to a division by zero in the Nernst-Planck equations
    T =  c[i][1]+273.15  # Temperature in Kelvin [K]
    N =c[i][1]   # OH- flux measured from experiment [mol/(cm2*s)]
    Cs1 = c[i][2]  # NaOH concentration in distilled water [mol/cm3]
    deltaC =c[i][3]  # difference of concentration between solutions [mol/cm3]
    # deltaC = Cs0 - 2*Cs1 --> because for 1 mol that is passing in the second compartment, the difference of concentration decrease of 2 mols
```

```
    #we feed the solver with the excel data of only 4 columns (for each test), that change at each second (each excel row)

    #Find the roots of a function
    #https://docs.scipy.org/doc/scipy/reference/generated/scipy.optimize.fsolve.html
    x0=[1e-9, 1e-10] #--> The starting estimate for the roots of func(x) = 0
    #xtol=1 --> The calculation will terminate if the relative error between two consecutive iterates is at most xtol.


    root = fsolve(func, x0, xtol=1)
    #fsolve uses a hybrid alghoritm to find roots


    #Non-linear solver (using initial guess value already found)
    #root = optimize.newton_krylov(func, x0, x_tol=1)
    #root = optimize.anderson(func, x0, x_tol=1)
    #root = optimize.broyden1(func, x0, x_tol=1)
    #root = optimize.broyden2(func, x0, x_tol=1)
    #root = optimize.excitingmixing(func, x0, x_tol=1)
    #root = optimize.linearmixing(func, x0, x_tol=1)
    #root = optimize.diagbroyden(func, x0, x_tol=1)

    #spy.optimize.minimizeci
    #https://docs.scipy.org/doc/scipy/reference/generated/scipy.optimize.minimize.html
    #Nelder-Mead
    #result1 = minimize(rosen, x0, method='Nelder-Mead', tol=1)
    #root = result1.x

    #BFGS
    #result1 = minimize(func, x0, method='BFGS', jac=derivative, options={'gtol': 1e-8, 'disp': True})
```

```
#result1


#Powell
#result1 = minimize(func, x0, method='Powell', jac=derivative, options={'gtol': 1e-8, 'disp': True})
#result1
#result1 = minimize(func, x0, method='Powell', jac=rosen_der, options={'gtol': 1, 'disp': True})
#root = result1

#CG
#result1 = minimize(func, x0, method='CG', jac=rosen_der, tol=1)
#root = result1.x

#Newton-CG
#bnds = ((0, None), (0, None)) #variables must be positive
#root = minimize(func, x0, method='Newton-CG', jac=derivative, bounds=bnds)



#L-BFGS-B
#root = minimize(func, x0, method='L-BFGS-B', jac=rosen_der)

#TNC
#root = minimize(func, x0, method='TNC', jac=rosen_der)

#COBYLA
#root = minimize(func, x0, method='COBYLA', jac=rosen_der)

#SLSQP
#root = minimize(func, x0, method='SLSQP', jac=rosen_der)

#trust-constr
```

```
    #root = minimize(func, x0, method='trust-constr', jac=rosen_der)

    #dogleg
    #root = minimize(func, x0, method='dogleg', jac=rosen_der, hess=rosen_hess)

    #trust-ncg
    #root = minimize(func, x0, method='trust-ncg', jac=rosen_der, hess=rosen_hess)

    #trust-exact
    #root = minimize(func, x0, method='trust-exact', jac=rosen_der, hess=rosen_hess)

    #trust-krylov
    #root = minimize(func, x0, method='trust-krylov', jac=rosen_der, hess=rosen_hess)



    writer1.writerow(root)
    #writer3.writerow(e) #the excel file of the writer 3 is overwritten with the new results

print("Done")
f.close()
#q.close()
```

B.2.2 Python code explanation

Here are some bullet points regarding the previous code:

- The code was built in the environment Spyder 4.0.1 of Anaconda (there should be no problem to run it also in an upgraded version of Spyder)
- two implicit equations were created with the two Nernst-Planck equations, so founding the diffusivities for each row, using a finding root method of a function intersecting the x-axis
- from all the measured excel file, sub-excel files for each test were created, with only 4 columns with T [C], N [mol/(cm^2*s)], Cs1 [mol/cm^3] and deltaC [-]. These values will be changed at each row of the iteration, Psi will be updated from these values, and all the others are constant
- the concentration gradient and the Psi were linearized, to consider only the difference at the two sides of the membrane, so using the boundary condition at x=0 and x=thickness (it is not so interesting having all the variation with position inside the membrane. The complete formulas of psi(x) and Cs(x) are available in the theoretical model of this thesis)
- the standard command to find the roots of an equation was used, they were double-checked the results with 11 different sets of excel data. To have an additional validation of the results (so to have also a third level of validation of the model) it is possible to activate the different non-linear methods written in the code (but left in comments, to not be read by the active code)